THE MOLECULAR BASIS FOR ALLOSTERIC CONTROL OF *ESCHERICHIA COLI* GLYCEROL KINASE BY FRUCTOSE 1,6-BISPHOSPHATE AND IIA^{GLC}

A Thesis

by

SHANNA QUINN MAYOROV

Submitted to the Office of Graduate Studies of
Texas A&M University
in partial fulfillment of the requirements for the degree of

MASTER OF SCIENCE

December 2011

Major Subject: Biochemistry

The Molecular Basis for Allosteric Control of *Escherichia coli* Kinase by Fructose 1,6-Bisphosphate and IIA^{glc}

THE MOLECULAR BASIS FOR ALLOSTERIC CONTROL OF ESCHERICHIA COLI GLYCEROL KINASE BY FRUCTOSE 1,6-BISPHOSPHATE AND IIA^{GLC}

A Thesis

by

SHANNA QUINN MAYOROV

Submitted to the Office of Graduate Studies of
Texas A&M University
in partial fulfillment of the requirements for the degree of

MASTER OF SCIENCE

Approved by:

Chair of Committee,	Donald W. Pettigrew
Committee Members,	David Peterson
	Frank Raushel
	Tatyana Igumenova
Head of Department,	Gregory Reinhart

December 2011

Major Subject: Biochemistry

ABSTRACT

Molecular Basis for Allosteric Control of *Escherichia coli* Glycerol Kinase by Fructose 1,6-Bisphosphate and IIA^{glc}. (December 2011)

Shanna Quinn Mayorov, B.S., Chemistry, Bloomsburg University

Chair of Advisory Committee: Dr. Donald Pettigrew

There has been progress towards elucidating the mechanism of *Escherichia coli* glycerol kinase (EcGK) control by its allosteric effectors fructose-1,6-bisphosphate (FBP) and IIA^{glc} (a member of the phosphoenolpyruvate:glycose phosphotransferase system). Determining the mechanism requires analysis of the interaction between these effectors and the substrates of EcGK. In this study, a structural and kinetic approach was used to determine inhibition by both the effectors. For this work, the use of fluorescence anisotropy to observe ligand binding was investigated. Also, a foundation was laid for future NMR experiments with EcGK.

For fluorescence studies, E36C EcGK was labeled with fluorescein and tested for changes in anisotropy in the presence of different ligands. To ensure that E36C was an appropriate representative of wildtype protein, initial velocity, inhibition, and heterotropic coupling assays were performed. Groundwork for future NMR experiments required analyzing substitutions of the native EcGK cysteines by initial velocity and inhibition studies.

By comparing wildtype enzyme and E36C (variant of wildtype with an engineered cysteine residue at position 36), it was found that E36C is a suitable substitute and was not drastically affected by labeling with fluorescein. Anisotropy values differed upon binding of different ligands and enabled titrations of the enzyme substrate complexes with both effectors to obtain dissociation constants. This supports using the stopped-flow method to assess the on- and off- rates of substrates and to obtain values for Q coupling. Furthermore, the results for FBP showed that inhibition by FBP is K-type (affects affinity) with respect to ATP and V-type (affects enzyme velocity) with respect to ADP. The findings presented also showed that native cysteine substitutions effect some of the catalytic and allosteric parameters of EcGK and would be powerful reporters for ligand binding in NMR. However, the enzymes are unstable and new protocols for protein isolation will need to be drafted.

DEDICATION

I dedicate this work to my loving husband Dmitriy Mayorov. He has been with me through all the sweat and tears and never ceased believing in my capabilities.

ACKNOWLEDGEMENTS

I thank my research supervisor and committee chair, Dr. Donald Pettigrew, for his guidance, support, and understanding. Not only has he helped me achieve my academic goals at Texas A&M, he has been a pillar of support for me personally. I thank my committee members, Dr. Peterson, Dr. Raushel, and Dr. Igumenova, for dedicating their time, energy, and support for me. I also express thanks to Frank N. Raushel for helping with the determination of some of the inhibition parameters in this work.

I am thankful for all the encouragement from the staff and my colleagues at Texas A&M University. I wish everyone the best of luck in their future endeavors and will remember you always.

NOMENCLATURE

6IAF	6-iodoacetamidofluorescein
β-Me	β-mercaptoethanol
DHAP	Dihydroxyacetone Phosphate
DMSO	Dimethyl Sulfoxide
DTT	Dithiothreitol
EAB	Enzyme/ATP/Gol Ternary Complex
EcGK	*E. coli* Glycerol Kinase
EPQ	Enzyme/ADP/G3P Ternary Complex
G3P	Sn-Glycerol-3-Phosphate
Glc	Glucose
Gol	Glycerol
IIA^{glc}	Glucose-Specific Phosphocarrier of the PTS System
IPTG	Isopropylthiogalactoside
NAD(H)	Nicotinamide Adenine Dinucleotide
NADP(H)	Nicotinamide Adenine Dinucleotide Phosphate
PTS	Phosphotransferase System
SDS-PAGE	Sodium Dodecyl Sulfate Polyacrylamide Gel Electrophoresis
TEA	Triethanolamine
WT	Wildtype EcGK

TABLE OF CONTENTS

CHAPTER Page

LIST OF FIGURES

FIGURE Page

LIST OF TABLES

CHAPTER I

INTRODUCTION

Although intensively studied, the molecular basis for allosteric control of proteins is poorly understood. Useful approaches for addressing allosteric regulation of proteins include enzyme kinetics and biophysical methods. By focusing on conformational changes at specific loci, these approaches may be used to probe the molecular basis for allosteric control. *Escherichia coli* glycerol kinase (EcGK) is one such system where limited knowledge of allosteric control exists. The employment of the aforementioned methods will be used to understand the basis for allosteric regulation of EcGK by examining effects at specific loci.

EcGK is a member of the sugar kinase/actin/hsp 70 superfamily, sharing some structural and catalytic properties with superfamily members (1). Within the superfamily, there is a conserved two domain structure. Each domain has two subdomains denoted IA/IB and IIA/IIB (Figure 1). The IA/IIA interface forms the conserved catalytic site for ATP hydrolysis associated with superfamily function (1). This catalytic cleft serves as the binding site for substrates, is formed by a conserved βββαβαβα topology in each subdomain, and is suggested to close through a shear motion (2) once substrates are bound (1,3-5). The divergent B subdomains form dimers from

---

This thesis follows the style of the *Journal of Biological Chemistry.*

junction of the IIB subdomains of two monomers. Interaction between IB subdomains of two dimers produces the enzyme tetramer form of EcGK. In addition to catalytic and structural similarities, EcGK and many members of the superfamily are subjects of allosteric control.

Allosteric effectors regulate enzyme catalysis in response to environmental stimuli. In the case of EcGK, the absence of glucose and simultaneous presence of glycerol triggers up-regulation of the glycerol kinase gene (*glpK*) (6-7). Without the presence of an effector, the enzyme catalyzes the rate-limiting step of glycerol metabolism by directly transferring the γ-phosphoryl of ATP to glycerol (8-12). The resulting product is Sn-glycerol-3-phosphate (G3P). G3P is converted to dihydroxyacetone phosphate (DHAP), an intermediate in the glycolytic pathway, and thus enables continuation of glycolysis. Glucose introduction to the cellular environment diminishes the necessity for glycerol metabolism and allosteric effectors inhibit EcGK enzyme catalysis (13-14).

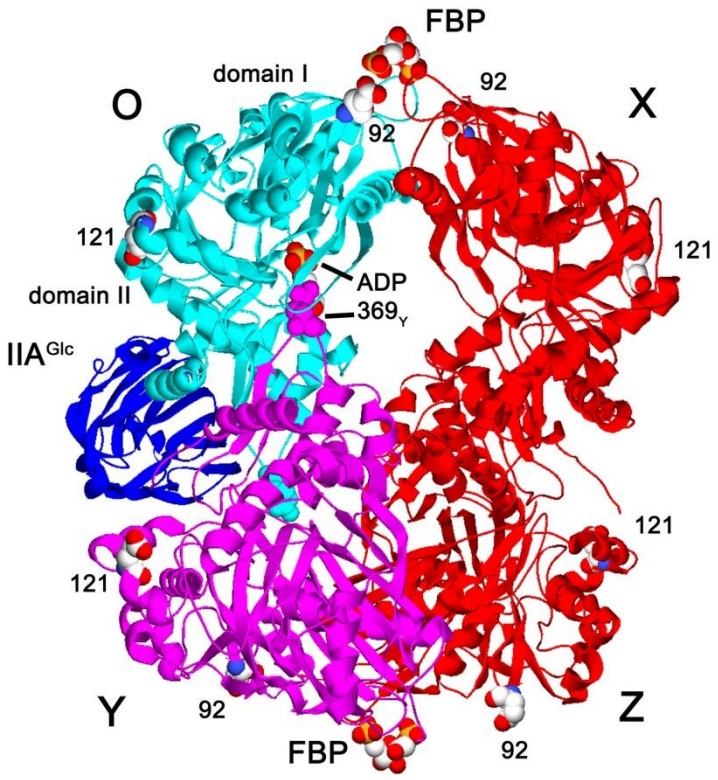

Figure 1: Ribbon Diagram of the EcGK Tetramer. The subunits are labeled as OXYZ. Each monomer has a domain I and domain II. The A subdomains form the catalytic cleft around ADP in the diagram and the B subdomains form oligomeric interactions between O/Y, O/X, Z/Y, and Z/X. The inhibitors FBP and IIA^{glc} bind to domain I and II, respectively. R369 is the oligomeric domain bridging residue that extends from one subunit into the catalytic cleft of the other in the dimer: R369 from the Y subunit extends into the O subunit.

Two different allosteric effectors, FBP and IIA^{glc}, control the catalytic activity of EcGK by binding to different domains (Figure 1). Binding to domain I is FBP, an intermediate in glycolysis that is a reporter for sugar availability, much like IIA^{glc}. IIA^{glc}, a member of the phosphoenolpyruvate:glycose phosphotransferase system (PTS) involved in cellular uptake of PTS sugars like glucose, binds to domain II of EcGK (15). Availability of PTS sugars reduces phosphorylation of IIA^{glc} histidine 90, enabling IIA^{glc} to assume an inhibitory role of glycerol kinase (5,16-17). Inhibition by allosteric

effectors such as FBP and IIA^{glc} is characterized as either V-type or K-type, where inhibition is with respect to a change in V_{max} or K_m, respectively. The first effector, FBP, has been shown to have characteristics of a V-type system (13). The second effector, IIA^{glc}, controls EcGK via V-type inhibition (18). Since both these effectors bind distal to the catalytic site in different domains, the question of how they elicit inhibition, and the conformational changes involved, is raised.

As seen for FBP and IIA^{glc}, allosteric control results from an effector molecule binding to one site and changing the function at another (19). Currently there exist two models of allosteric control mechanisms. The traditional model attributes control to conformational changes in quaternary structure that affect binding or catalysis (20-21). More recently, exertion of control is being attributed not to global effects, but to perturbations of sparse amino acid networks (22-23). By analyzing conformational changes that result from FBP and IIA^{glc} binding, identification of EcGK with one of these two models is possible.

Analysis of the crystal structures of wildtype EcGK and its variants has not elucidated the mode of allosteric control by FBP or IIA^{glc}. From these crystal structures, however, it was proposed in 1993 that control could be attributed to R369, an amino acid near the cleft opening that interjects from one subunit into the neighboring subunit (Figure 1)(15). This interjection holds the amino acid within 10Å of the nucleotide ADP in the neighboring subunit. Support for R369 importance in allosteric regulation was found in 2009, where truncation to an alanine reduced inhibition by IIA^{glc} (18).

Based on the above observation, the arginine peg (R369) and its interaction with neighboring residues in both domains were inspected. Two of the three amino acids involved in these domain bridging interactions were Q37 and Y39 of domain I. These amino acids are within 3.5Å of the arginine guanidinium group and affect the FBP/IIA^{glc} inhibition parameters and the EcGK Michaelis constants. A previously generated Q37A substitution exhibited a decreased V_{max}, decreased affinity for IIA^{glc}, decreased affinity for FBP, and decreased inhibition by FBP (24). A previously generated Y39A substitution exhibited a decreased V_{max}, decreased affinity for ATP and glycerol, abolished IIA^{glc} inhibition, and decreased the affinity for FBP (24).

Position E36 is located on the same small mobile loop as Q37 and Y39 near the cleft opening of both the *E. coli* and *E. casseliflavus* glycerol kinases (Figure 2). It has been further shown that glycerol binding to *E. casseliflavus* glycerol kinase induces a conformational shift in amino acid positions 36-48 (25). For EcGK, crystal structures of variants sample different conformations in this region, as shown in S58W and G230C (26-27).

It is possible that an E36 variant may further elucidate the role of this loop in allosteric control. The mobile loop containing E36 (Figure 2) is solvent accessible and is a prime target for fluorescence studies. By labeling the engineered cysteine at position 36 with the fluorescent probe 6IAF, it may be possible to determine the effect of ligand binding on conformational changes at this locus from changes in anisotropy or intensity. This E36C variant was previously constructed and shown to be specifically labeled by 6IAF (28). Since it was recently discovered that binding of ATP affects E36C

anisotropy, it is expected that other ligands may affect the fluorescence properties of E36C as well (29). To prepare for these studies, the effects on the catalytic and allosteric parameters of the E36C substitution, as well as the effect of labeling at this position, was determined. After determining how the substitution and labeling affect the enzyme, the effect of substrate and inhibitor binding on fluorescence was examined.

A second approach to determining inhibitor effects on substrate binding is by NMR spectroscopy. NMR spectroscopy has been used in the scientific literature to analyze molecular motions. Because of its versatility and capabilities to examine the microscopic environment surrounding individual residues, it is an extremely useful tool. Until recently, NMR was mainly used to study enzymes less than 35 kDa (30). *E. coli* glycerol kinase is a tetrameric protein of 56 kDa per subunit, much too large for conventional NMR studies. Recently, however, there have been innovations within the field that allow examination of larger structures by using solid state NMR. This method has no inherent limitations on protein size as orientation averaging can be mimicked and reduces the effect on tumbling rate.

To use solid state NMR, many researchers use site specific isotopes and analyze the environment around these key points in the protein. One ideal target for isotope labeling is the amino acid cysteine. There are five native cysteines in EcGK that are well distributed throughout the protein (Figure 2). These residues are potential probes for analyzing ligand binding effects on EcGK conformational changes. If substitutions at these positions alter the catalytic or allosteric properties of EcGK, then the affected cysteine should be a useful reporter for ligand binding by NMR. By determining the

effects of native cysteine substitutions on the catalytic and allosteric properties of EcGK, it is possible to predict which of these loci will report on inhibition.

Figure 2: Crystal Structure Showing Native Cysteines and Position E36. The image is a homodimer with its secondary structure shown in ribbon form and colored pink for α-helices, orange for β-sheets, and purple for turns. The ball and stick structure in the catalytic cleft of each subunit is an ATP analog. The five native cysteine residues are shown in green on each subunit. Position E36 is shown in cyan. This image is from PDB: 1GLL.

The above mentioned specific loci in EcGK have the potential to report on ligand induced conformational changes. By labeling an engineered cysteine at E36 with

fluorescein it is possible to examine ligand induced structural changes by fluorescence. This approach will enable determination of the mechanism of allosteric control for FBP and IIA^{glc} by analyzing their effects on substrate binding. In this study, the effect of the E36C substitution is characterized, anisotropy dependence of labeled E36C in the individual and simultaneous presence of ligands is assessed, and the applicability of the using the native cysteine substitutions as reporters for inhibition is determined

CHAPTER II

SPECIFIC AIMS

The key goals of this work are shown below in order of assessment:

1.) Determine Effect of the E36C Substitution and Its Labeling on the Catalytic and Allosteric Properties of EcGK.

2.) Define the Effect of Ligand Binding on the Fluorescence Properties of 6IAF Labeled E36C.

3.) Evaluation of the Potential Use of EcGK Native Cysteines as Probes for Ligand Induced Conformational Changes.

CHAPTER III

MATERIALS AND METHODS

Materials

General. All chemicals and enzymes, with the exception of *E. coli* glycerol kinase and IIA^{glc}, were purchased from Sigma-Aldrich Chemical Co. (St. Louis Missouri), unless specified. To perform SDS-PAGE, reagents were purchased from Thermo Fisher Scientific. All centrifugations were performed using the Sorvall RC-5B Superspeed Centrifuge with the Fiberlite F15S-8X50C rotor at $4^{o}C$ unless otherwise specified. Sonication was performed using W220-F Sonicator with microtip from Heat Systems-Ultrasonics Inc. All enzyme assays and protein concentration determinations were performed using the Beckman UV/VIS DU800 Spectrophotometer.

Glycerol-3-Phosphate Purification and Concentration Determination. Glycerol-3-phosphate (G3P) was purchased as a cyclohexammonium salt. Exchange of the cyclohexammonium salt for sodium was performed on a cation exchange column (1.2 x 5.7 cm) with AG50W-X4 hydrogen form resin from BioRad. A total of 0.67 mmol of G3P-cyclohexammonium salt was loaded onto the column and eluted using milliQ H_2O to remove the cyclohexammonium salt. The first 2 mL of flow through were discarded and the subsequent 3 mL collected and tested for G3P concentration.

To determine the concentration of G3P in the collected 3 mL volume, a set of 0.5 mL assays composed of "reverse cocktail" (40 mM Triethanolamine-HCl buffer pH 7.0, 10 mM $MgCl_2$, 14.7 units of glucose-6-phosphate dehydrogenase, 29 units of

hexokinase, 2 mM D-glucose, and 0.2mM $NADP^+$), 2.5 mM ADP, and 90 μg/mL EcGK were prepared (see the activity scheme in Figure 3). Each assay was measured for its A_{340} reading before adding any of the G3P solution. This was recorded as the starting point for determining the total change in absorbance. At this time, a sample of the G3P solution was added and the reaction allowed to continue until completion. One cuvette had deionized water added in lieu of G3P and served as the control. Using Beer's Law and the extinction coefficient of 6.2 $mM^{-1}cm^{-1}$ for NADPH, the concentration of G3P was determined. This is because one G3P molecule is consumed for every NADPH molecule generated. All measurements were performed on the Beckman UV/VIS DU800 Spectrophotometer.

$$ADP + G3P \xrightarrow{EcGK} ATP + Gol$$

$$ATP + Glc \xrightarrow{HK} ADP + Glc - 6 - Phosphate$$

$$Glc - 6 - Phosphate + NADP^+ \xrightarrow{G6PD} 6 - P - gluconate + NADPH$$

Figure 3: Representation of Continuous ATP Assay. The coupling enzymes, HK (hexokinase) and G6PD (glucose-6-phosphate dehydrogenase), are added in the enzyme assay at 29 units and 14.7 units per 0.5mL, respectively, to enable visualization of the reverse reaction from monitoring NADPH levels. *Glc* stands for glucose.

Enzyme Purification

IIA^{glc} Purification. The protein IIA^{glc} was expressed in *E. coli* BL21 DE3 cells using the pVEX-crr plasmid and purified as previously described (31). This plasmid was provided by Dr. Saul Roseman, Department of Biology, Johns Hopkins University (Baltimore MD). The concentration of the protein was determined by measuring the A_{260} with an extinction coefficient of 1.6 $mM^{-1}cm^{-1}$ (5).

EcGK Purification. For purification of wildtype EcGK, the protein was expressed using either the pHG165 plasmid as previously described (32) or the pET28 plasmid, which confers kanamycin resistance. The sample was then sonicated and treated with streptomycin sulfate, two treatments of ammonium sulfate, a Q Sepharose Fast Flow column (pH 8.0), Source 15Q pH 7.0, and Source 15Q pH 8.0 as described in (28,33). When using the pET28 plasmid, the antibiotic used to select for transformants was kanamycin at 50 μg/mL.

The E36C and cysteine substitutions were all previously constructed using the pHG165 plasmid and were isolated as above (28). E36C went through the above mentioned steps and an additional ATP agarose column as previously described (28,33). This final column was (1.5 cm x 4 cm) and had an ATP C-8 matrix attachment (catalog: A2767). E36C was eluted by 1 mM ATP in 0.05 M NaCl glpK standard buffer pH 7.0 (standard buffer composition: 50 mM triethanolamine (TEA), 2 mM glycerol, 1 mM EDTA, 2 mM mercaptoethanol, adjusted to either pH 8.0 or 7.0) (34).

At the end of EcGK purification, the presence of EcGK was confirmed by an enzymatic assay and analyzed for purity by SDS-PAGE. The concentration of EcGK was determined by using an extinction coefficient of 1.73 $(mg/mL)^{-1}cm^{-1}$(33). Both E36C and EcGK were stored as crystalline suspensions in ammonium sulfate and stored at $4^{o}C$ as previously described (35).

Initial Velocity, Inhibition, and Coupling Studies

Enzyme Preparation. Prior to experimentation, EcGK crystals underwent a buffer exchange by passing through a NAP-10 mini-column equilibrated with glpK standard buffer pH 7.0 or 0.1 M TEA pH 7.0. The 0.1 M TEA buffer was used when varying glycerol concentration or working with the enzyme/G3P/ADP complex. Crystalline EcGK was re-suspended in 1 mL of the chosen buffer from above and loaded onto the equilibrated mini-column and the flow-through discarded. The sample was eluted with 1.4 mL of the same buffer used to equilibrate the column and tested for protein concentration using an extinction coefficient of 1.73 $(mg/mL)^{-1}cm^{-1}$(33).

Enzyme Catalytic Activity Assays (Forward Direction). Enzyme activity was analyzed in the forward direction (ATP/Gol) by monitoring the decrease of NADH concentration via ΔA_{340} with the extinction coefficient 6.2 $mM^{-1}cm^{-1}$. Activity is measured by a continuous ADP-coupled spectrophotometric assay at pH 7.0 and at 25 ^{o}C, as shown in Figure 4. Each 0.5 mL assay contains "forward cocktail" (50 mM triethanolamine-HCl (TEA) buffer, 5 mM $MgCl_2$, 20 mM KCl, 7.5 units of pyruvate kinase, 7.5 units of lactate dehydrogenase, 0.2 mM PEP, 0.2 mM NADH), and 0.5 μg/mL EcGK.

$$ATP + Gol \xrightarrow{EcGK} ADP + G3P$$
$$ADP + PEP \xrightarrow{PK} ATP + Pyruvate$$
$$Pyruvate + NADH \xrightarrow{LDH} Lactate + NAD^{+}$$

Figure 4: Representation of Continuous ADP Assay. PK stands for pyruvate kinase, LDH stands for lactate dehydrogenase, and Gol is glycerol. As EcGK converts Gol to G3P, ADP is produced. As the concentration of ADP increases, PK converts it back to ATP using PEP. This reaction serves a two-fold purpose. First it retains the solution concentration of ATP in the cuvette and second it provides pyruvate, which is the substrate for LDH. LDH then converts pyruvate and NADH to lactate and NAD^{+}. It is this conversion that can be visualized on the spectrophotometer. Therefore, for each ATP molecule consumed, one NADH molecule is consumed.

When determining the Michaelis constant for ATP, 10 mM glycerol was added to each 0.5 mL assay and ATP was varied from 0.5-100 μM. Varying the ATP concentration up to 100 μM saturates the first of two binding sites on EcGK, which is the most accurate for kinetic parameter determination (34). When determining the Michaelis constant for glycerol, 2.5 mM ATP was added to each 0.5 mL assay and glycerol was varied from 5-1600 μM. The assays were initiated by addition of the EcGK enzyme to the final concentration of 0.5 μg/mL. To obtain the Michaelis constants, the kinetic data were fit to the Michaelis-Menten equation (Equation 1) by using Kaleidagraph (Synergy Software, Reading, PA). In Equation 1, v_0 is the initial velocity at the indicated concentration of ATP, $V_{\max}$ is the maximum velocity of the enzyme at saturating substrate, $[ATP]$ is the concentration of ATP, and K_m^{ATP} is the Michaelis constant for ATP. The equation can be used for glycerol as well by changing all terms containing ATP to glycerol.

$$v_0 = \frac{V_{\max}[ATP]}{[ATP] + K_m^{ATP}} \quad (1)$$

Enzyme Catalytic Activity Assays (Reverse Direction). Enzyme activity was analyzed in the reverse direction (ADP/G3P) by monitoring the increase of NADPH concentration via ΔA_{340} with the extinction coefficient of 6.2 $mM^{-1}cm^{-1}$. This ATP-coupled spectrophotometric assay is measured at pH 7.0 and 25 ^{o}C, activity scheme is in Figure 3. Each 0.5 mL assay contained the reverse cocktail components and 8.5 μg/mL EcGK.

When determining the Michaelis constant for ADP, 2.5 mM G3P was added to each 0.5 mL assay and ADP was varied from 0.1-0.5 mM. When determining the Michaelis constant for G3P, 0.5 mM ADP was added to each 0.5 mL assay and G3P was varied from 0.05-0.6 mM. The assays were initiated by addition of the EcGK enzyme. To obtain the Michaelis constants, the kinetic data were fit to Equation 1 above (switch out ATP for ADP and Gol for G3P) using the Kaleidagraph Synergy software.

FBP/IIA^{glc} Inhibition Assays. All inhibition assays had the same components in the 0.5 mL assay as the catalytic assays described above, depending on which direction the enzyme was being tested. Forward direction: forward cocktail, 2.5 mM ATP, 10 mM glycerol, and EcGK at a final concentration of 0.5 μg/mL. Reverse direction: reverse cocktail, 0.5 mM ADP, 2.5 mM G3P, and EcGK at a final concentration of 8.5 μg/mL. The allosteric effector concentrations were varied as shown in the figures.

For FBP inhibition each assay was incubated for 45 minutes with all assay components, including EcGK, with the exception of ATP/ADP. The nucleotide was used to initiate the reaction. For IIA^{glc} inhibition, the enzyme was added to initiate the reaction.

Allosteric inhibition of EcGK is shown in the context of the thermodynamic linkage scheme in Figure 5. The two key allosteric parameters that are defined from this scheme are shown in Equations 2 and 3. The first parameter is W, which describes the effect of the inhibitor on the V_{max} of the enzyme. The second parameter is Q, which describes the mutual effect of the substrate and the inhibitor on binding.

Two kinetic parameters elucidated from inhibition studies are $K_{0.5}$ and W. These parameters are elucidated from the thermodynamic linkage scheme in Figure 5. $K_{0.5}$ is the apparent dissociation constant for effector binding. This parameter reflects the K_d for IIA^{glc} because IIA^{glc} binding occurs through a single binding event (see Equation 2). In this equation, W is the coupling parameter that describes the effect of the inhibitor on V_{max} for either FBP or IIA^{glc}, SA_0 is the specific activity in the absence of inhibitor and SA_∞ is the specific activity in the saturating presence of inhibitor, V^∞ is the maximum velocity in the saturating presence of inhibitor, and V^0 is the maximum velocity in the absence of inhibitor. The ratio of the SA or V_{max} in the saturating presence of inhibitor to the SA or V_{max} in the absence of inhibitor is W. When W>1, there is activation by the allosteric effector. When W<1, there is inhibition. When W=1, there is no allosteric effect on V_{max}. This equation can be used for either FBP or IIA^{glc}. The allosteric inhibitor FBP binds to two sites per EcGK tetramer and shows homotropic coupling.

Therefore, its $K_{0.5}$ is not equivalent to K_d and the homotropic coupling is expressed by the Hill coefficient (n_H) as shown in Equation 3. In Equation 3, the term Q is the coupling parameter that describes the effect of one ligand binding in the presence of another, K_A^0 = K_m for ATP in the absence of the inhibitor, K_A^∞ = K_m for ATP in the saturating presence of the inhibitor, the K_{II}^0 = $K_{0.5}$ for IIA^{glc} in the absence of substrate, K_{II}^∞ = $K_{0.5}$ in the saturating presence of substrate, and K_{FBP} = $K_{0.5}$ for FBP. When Q=1, there is no allosteric coupling, when it is greater than one there is cooperative coupling, and if it is less than one it is antagonistic.

The data from each experiment is therefore fit to these equations using a non-linear least squares fit with Kaleidagraph Synergy software. W is the coupling parameter that describes the effect of an inhibitor on V_{max} and can be used in Equation 4 to describe the effect of FBP and IIA^{glc}.

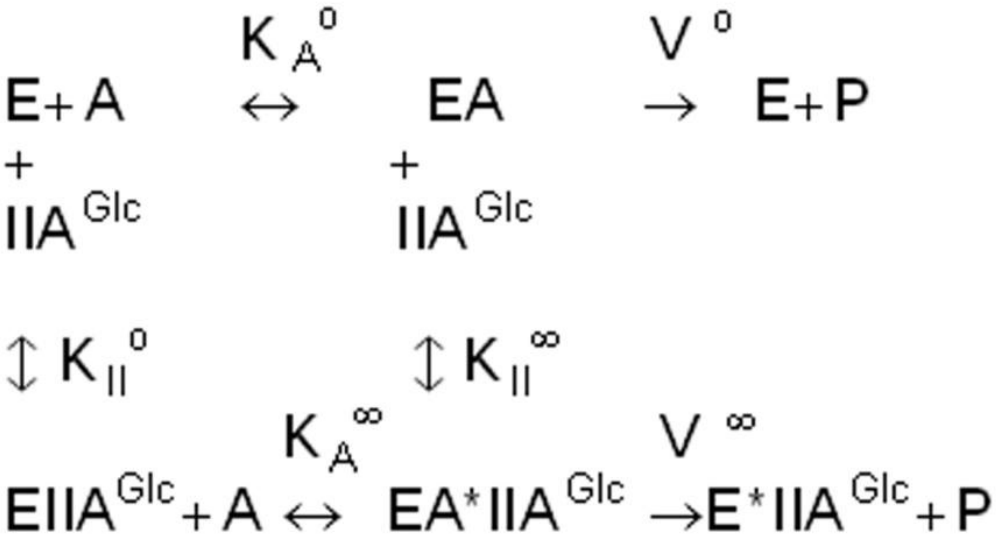

Figure 5: Thermodynamic Linkage Scheme Depicting Allosteric Coupling Between IIA^{glc} and Mg•ATP for EcGK. The term *E* represents either the enzyme/glycerol or enzyme/G3P complex. The term *A* represents either Mg•ATP or Mg•ADP. K_A^0 = K_m for ATP in the absence of the inhibitor and K_A^∞ = K_m for ATP in the saturating presence of the inhibitor. K_{II}^0 = $K_{0.5}$ for IIA^{glc} in the absence of nucleotides and K_{II}^∞ = $K_{0.5}$ in the saturating presence of nucleotides. V^∞ is the maximum velocity in the saturating presence of IIA^{glc} and V^0 is the maximum velocity in the absence of IIA^{glc}. *P* is product. The structure of the linkage scheme applies for FBP as well.

$$W = \frac{V^\infty}{V^0} = \frac{SA_\infty}{SA_0} \tag{2}$$

$$Q = \frac{K_A^0}{K_A^\infty} = \frac{K_{II}^0}{K_{II}^\infty} or \frac{K_{FBP}^0}{K_{FBP}^\infty} \tag{3}$$

Allosteric inhibition studies for FBP or IIA^{glc} are characterized by varying the inhibitor concentration at saturating concentrations of both substrates. The dependence

of the enzyme specific activity on the inhibitor concentration was fit to Equation 4 for IIA^{glc} inhibition and Equation 5 for FBP inhibition. W was calculated using Equation 2. The terms in Equation 4 are defined as follows: $SA_{[X]}$ is the specific activity at x concentration of inhibitor, SA_0 is the specific activity in the absence of inhibitor, SA_∞ is the specific activity in the saturating presence of inhibitor, $[X]$ is the concentration of inhibitor, and $K_{0.5}$ is the concentration of inhibitor that gives fifty percent of the maximum inhibition. This equation can be used to describe IIA^{glc} binding and inhibition. The terms in Equation 5 are defined as follows: $SA_{[X]}$ is the specific activity at x concentration of inhibitor, SA_0 is the specific activity in the absence of inhibitor, SA_∞ is the specific activity in the saturating presence of inhibitor, $[X]$ is the concentration of inhibitor, and $K_{0.5}$ is the concentration of inhibitor that gives fifty percent of the maximum inhibition. The term n_H is the Hill coefficient, which describes the effect of homotropic coupling for FBP. When n_H >1 there is cooperative coupling. When n_H <1 there is antagonistic coupling. When n_H =1 there is no coupling.

$$SA_{[X]} = SA_0 - \frac{(SA_0 - SA_\infty)[X]}{K_{0.5} + [X]} \tag{4}$$

$$SA_{[X]} = SA_0 - \frac{(SA_0 - SA_\infty)[X]^{nH}}{[K_{0.5}]^{n_H} + [X]^{nH}} \tag{5}$$

Heterotropic Coupling. For this measurement, the concentration of the nucleotide was varied at different fixed concentrations of inhibitor in the saturating presence of either glycerol or G3P. Assays were performed to ascertain the extent of coupling between nucleotide and allosteric effector binding. When analyzing coupling between FBP/IIA^{glc} and ATP, each 0.5 mL assay contained the forward cocktail components, 10 mM glycerol, and 0.5 μg/mL EcGK. ATP and the allosteric effectors FBP and IIA^{glc} were varied as shown in the figures. Each FBP containing assay was incubated with all assay components, including EcGK, for 45 minutes and was initiated with ATP. Each IIA^{glc} containing assay was initiated by adding EcGK.

To analyze coupling between FBP/IIA^{glc} and ADP, each 0.5 mL assay contained the reverse cocktail components, 2.5 mM G3P, and 8.5 μg/mL EcGK. ADP and the effectors FBP and IIA^{glc} were varied as shown in the figures. Each FBP containing assay was incubated with all assay components, including EcGK, for 45 minutes and was initiated with ATP. Each IIA^{glc} containing assay was initiated by adding EcGK.

Coupling parameters were obtained from these initial velocity enzyme kinetics studies from fits of the data to Equation 6 (for FBP) and Equation 7 (IIA^{glc}) using the EnzFitter program. The terms are described previously in Figure 5 for both equations

$$v_0 = \frac{V^0([ATP](K_{FBP}^0)^{n_H} + [ATP][FBP]^{n_H} QW)}{[ATP](K_{FBP}^0)^{n_H} + [FBP]^{n_H} K_A^0 + [ATP][FBP]^{n_H} Q + (K_{FBP}^0)^{n_H} K_A^0} \quad (6)$$

$$v_0 = \frac{V^0([ATP]K_{II}^0 + [ATP][IIA^{glc}]QW)}{[ATP]K_{II}^0 + [IIA^{glc}]K_A^0 + [ATP][IIA^{glc}]Q + K_{II}^0 K_A^0} \quad (7)$$

E36C Fluorescence Measurements

Preparing E36C for Labeling. A small volume of E36C ammonium sulfate crystal suspension was diluted to 0.990 mL in Sephacryl Buffer (0.1 M TEA pH 8.0, 2 mM glycerol). DTT was added to the sample to a final concentration of 10 mM in 1 mL, which was then incubated for thirty minutes at room temperature (this incubation period assures that all cysteines are completely reduced for subsequent labeling). Next, the sample was spun at 13,000 rpm for 1 min in a microcentrifuge to remove any precipitate. DTT and ammonium sulfate were removed from the sample by purification on a NAP-10 column pre-equilibrated with Sephacryl buffer. The flow-through was discarded and the sample eluted with 1.4 mL of Sephacryl buffer into a black 1.5 mL microfuge tube. The protein concentration was determined by measuring the A_{280}.

Labeling of E36C. After undergoing the buffer exchange described above, ATP was added to the sample at a final concentration of 2.5 mM. This addition of the nucleotide is necessary because it affects the conformation of the enzyme and protects native cysteines from conjugation with the fluorophore (28). At this point, 4750 μM 6-iodoacetamidofluorescein (6IAF) in DMSO was added at a concentration three times that of the protein concentration. The labeling reaction was incubated for 15 min and quenched by the addition of 1 μL of 1:10 β-mercaptoethanol (β-Me). Once quenched, the sample was concentrated to 1 mL using the Centricon® mini-concentrator by centrifugation at 5,000 rpm for 8 min. The concentrated sample was purified on a NAP-10 column pre-equilibrated with glpK standard buffer pH 7.0 to remove β-Me, 6IAF, and residual ATP. The flow-through was discarded and sample eluted with 1.4 mL of

glpK standard buffer pH 7.0. The sample was then dialyzed three times: four hours in 1 L of 0.2 M NaCl glpK standard buffer pH 7.0, overnight in 1 L of 0.1 M TEA pH 7.0, and four hours in 1L of 0.1 M TEA pH 7.0. The dialyzed sample was scanned from 260-600 nm and the A_{280} and A_{492} were recorded. The two absorbance values were used to determine the protein concentration and the stoichiometry of labeling (mol 6IAF/mol GK). Stoichiometries were required to be below 0.12 to prevent homo-FRET during fluorescence experiments (28). The sample was kept in a black microfuge tube at all times to protect the fluorophore from degradation.

Fluorescence Measurements. All steady-state anisotropy measurements were made at 25 ^{o}C using ISS Phoenix/SLM 4800 Spectrofluorometer with Vinci Software (2002-2005). The spectrofluorometer was equipped with Glan-Thompson calcite prism-type polarizers. The excitation wavelength used was 485 nm and the emission wavelength was collected using a 514.5 nm interference filter. All anisotropy measurements were calculated using by the Vinci software.

Equation 8 was used to extract the $K_{0.5}$ when performing titrations of 6IAF labeled E36C with FBP and IIA^{glc}. The terms used are defined as follows: $< r >_{[X]}$ is the anisotropy at X concentration of FBP, $< r >_0$ is the anisotropy in the absence of FBP, $[X]$ is the concentration of FBP used, $K_{0.5}$ is the concentration of FBP required to reach half saturation of the enzyme, and n_H is the Hill coefficient. When looking at the effects of IIAglc inhibition, the structure of the equation is the same, except $[X]$ and $K_{0.5}$ are not raised to the n_H.

$$< r >_{[X]} = \frac{(< r >_0)[X]^{nH}}{[K_{0.5}]^{n_H} + [X]^{nH}} \quad (8)$$

CHAPTER IV

RESULTS

Determining the Effect of the E36C Substitution and Its Labeling On the Catalytic and Allosteric Properties of EcGK

Purification of Wildtype and E36C EcGK. Glycerol kinase was isolated and purified from *E. coli* cells as described previously in the Materials and Methods section. Both wildtype and the E36C variant had similar ammonium sulfate solubility and eluted at the same position on the Source 15Q pH 8.0 and pH 7.0 columns, and on the Q-Sepharose Fast Flow column. SDS-PAGE of the column fractions from wildtype EcGK and E36C purification are shown in Figure 6. As can be seen from the gel images, the proteins are substantially homogeneous and were used for later experimentation.

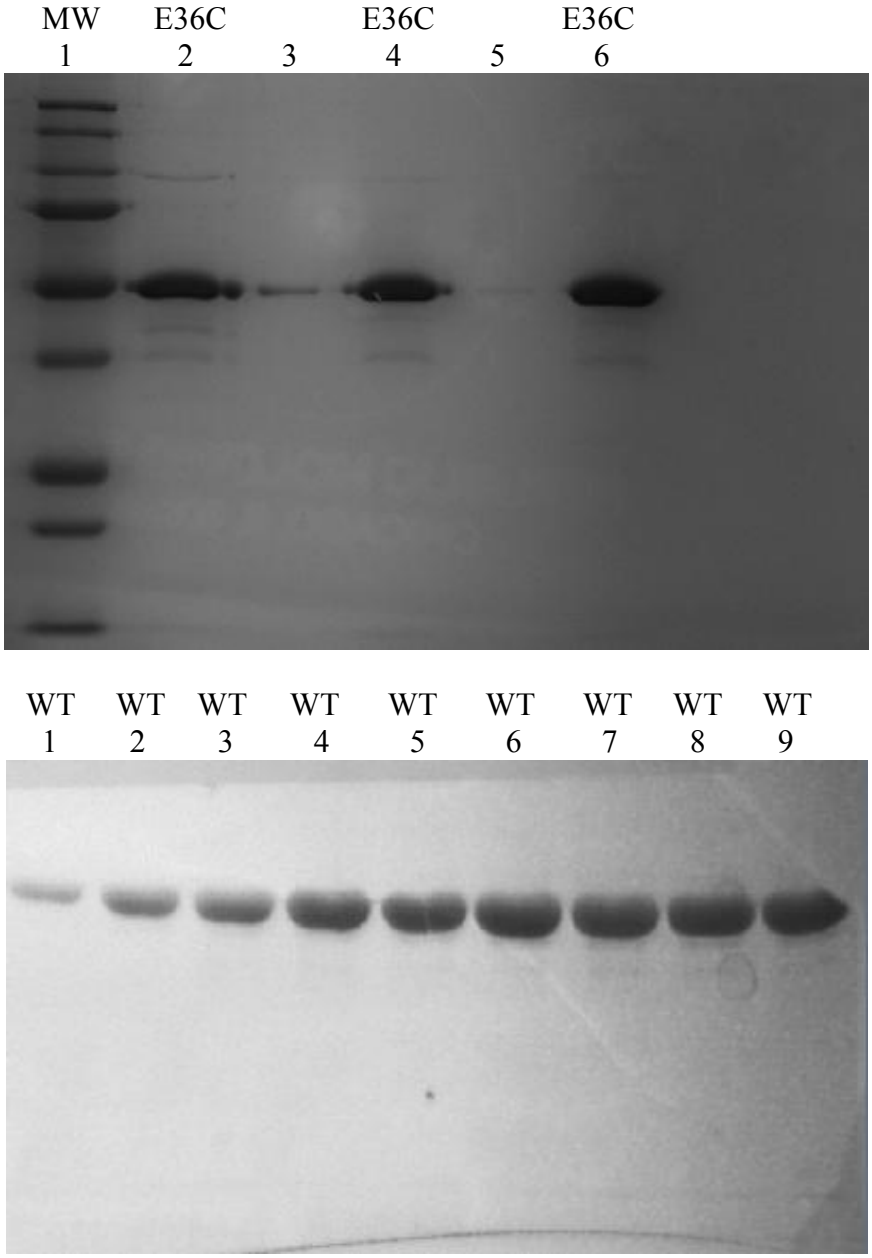

Figure 6: Purified E36C and Wildtype EcGK. The top gel is an 10% SDS-PAGE of E36C fractions after the ATP agarose column. The molecular weight marker is in lane 1: 250 kD, 150 kD, 100 kD, 75 kD, 50 kD, 37 kD, 25 kD, 20 kD, and 15 kD. The collected fractions are in 2, 4, and 6 and were pooled for future use. The artifacts in lanes 3 and 5 are overflow from the previous lane. The bottom gel is a 10% SDS-PAGE of wildtype EcGK after the Source 15Q column pH 8.0. Lanes 1 through 9 correspond to an individual fraction collected off the column and were all pooled for future use.

Wildtype and E36C Initial Velocity Studies. The kinetic parameters obtained for conversion of ATP/glycerol to ADP/G3P and ADP/G3P to ATP/glycerol between wildtype EcGK and the variant E36C were compared to ascertain the effect of this substitution. The assays were performed via the ADP and ATP coupling explained in the Materials and Methods section.

The data presented in this section are for G3P and glycerol K_m determination and those for ATP and ADP are presented later. To determine the K_m for glycerol, ATP was added to 2.5 mM and glycerol varied using the forward cocktail components described in the Materials and Methods section. To determine the K_m for G3P, ADP was added to 0.5 mM and G3P varied using the reverse direction cocktail components described previously. The dependence of the initial velocity on glycerol and G3P concentration is shown in Figures 7 and 8 below. The kinetic data obtained from these experiments were fit using Equation 1 in Kaleidagraph and compared in the table on page 40.

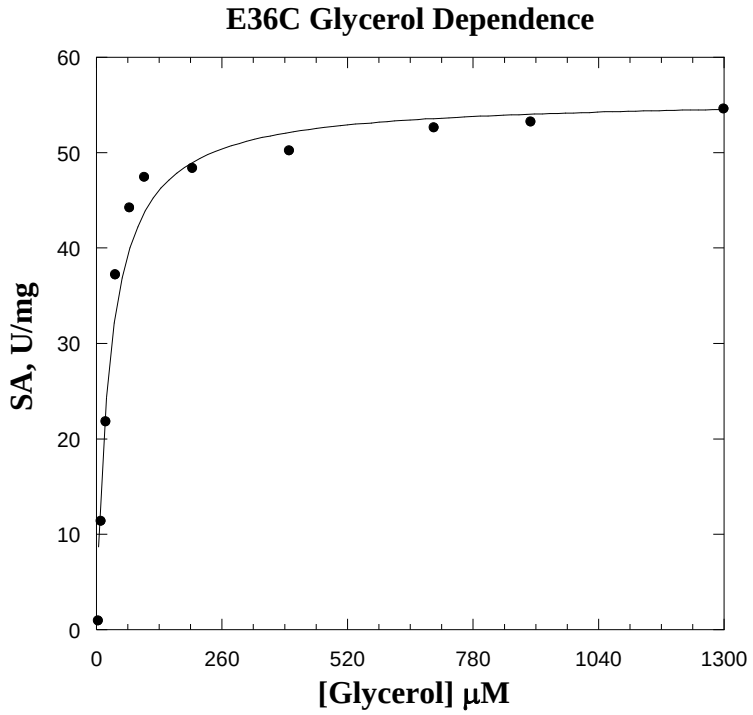

Figure 7: E36C Glycerol Dependence. Each point on the graph indicates an individual assay conducted at the indicated glycerol concentration. The line shows the fit to Equation 1. Each assay was initiated with enzyme that was added to a final concentration of 0.5 μg/mL.

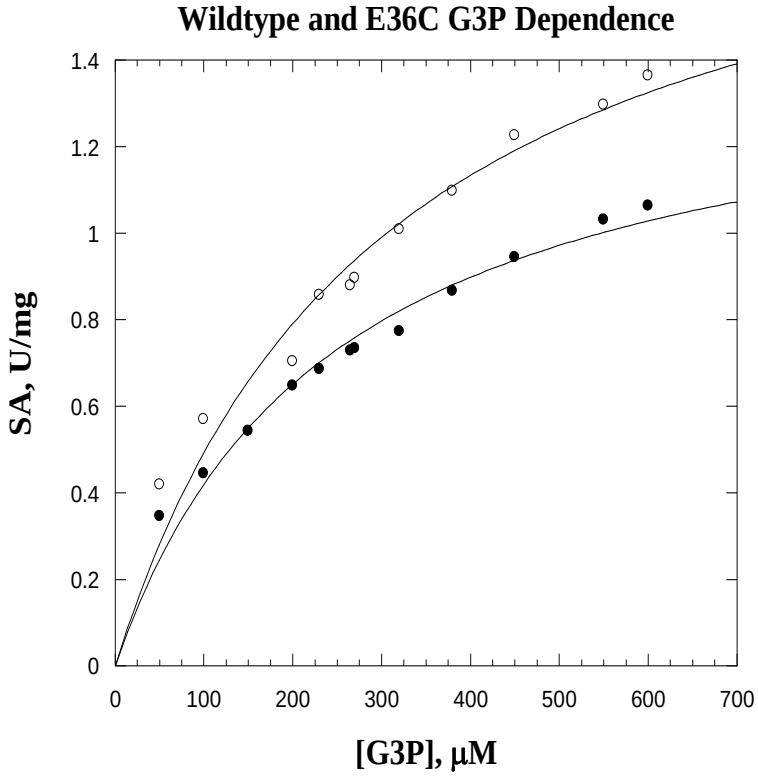

Figure 8: Wildtype and E36C G3P Dependence. Each point on the graph indicates an individual assay conducted at the indicated G3P concentration. The lines show the fits for each enzyme to Equation 1. The open circles represent wildtype and the filled circles represent E36C. The lines show the fit to Equation 1. Each assay was initiated with enzyme that was added to a final concentration of 8.5 μg/mL.

FBP Inhibition of Wildtype and E36C. To characterize the extent of inhibition of E36C compared to wildtype, inhibition studies were performed for both enzymes. The activity dependence as a function of FBP concentration for both enzymes is shown below in Figures 9 and 10. The fits were generated using Equation 5 which provided the parameters $K_{0.5}$ and n_H. The parameter W was determined using Equation 2. The results of inhibition of the forward reaction were compared to the published results for FBP (5)

and the results of inhibition in the reverse reaction were compared independently in this work. These values were compared in the table on page 40.

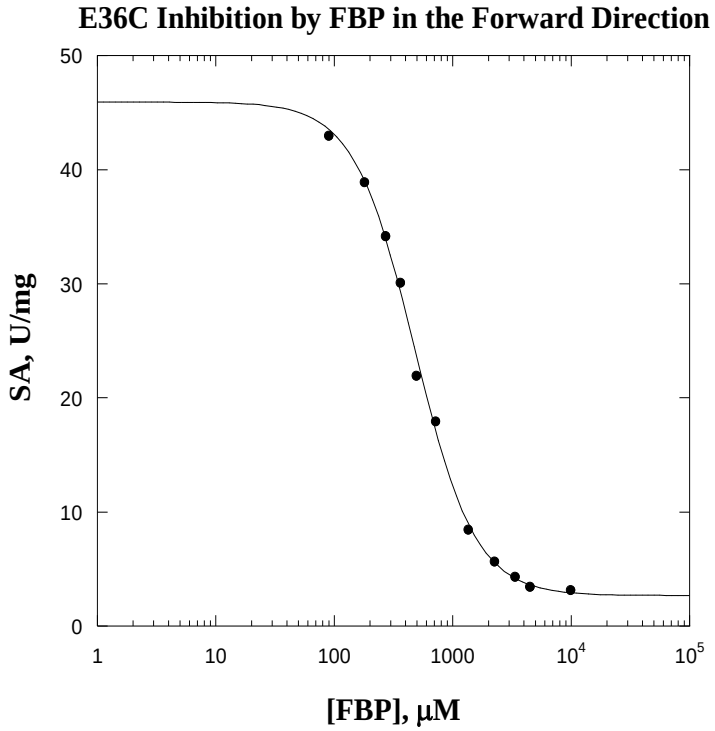

Figure 9: E36C Inhibition by FBP in the Forward Direction. Each point on the graph indicates an individual assay conducted at the indicated FBP concentration. The line shows the fit to Equation 5. The parameter W was determined using Equation 2. Each assay was incubated for 45 min and initiated with ATP at a final concentration of 2.5 mM.

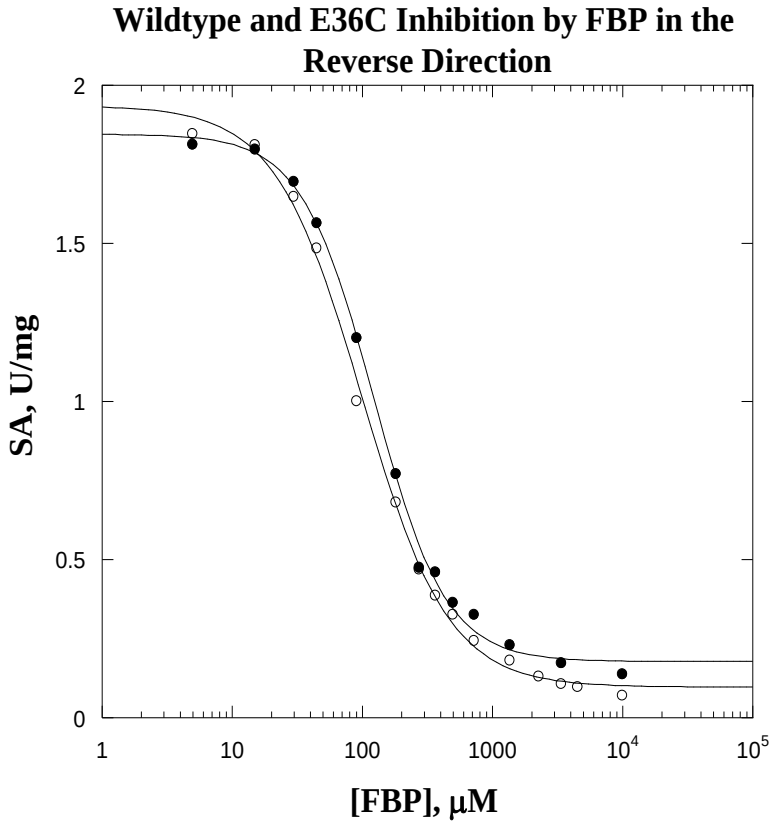

Figure 10: Wildtype and E36C Inhibition by FBP in the Reverse Direction. Each point on the graph indicates an individual assay conducted at the indicated FBP concentration. The open circles represent wildtype and the filled circles represent E36C. The line shows the fit to Equation 5. The parameter W was determined using Equation 2. Each assay was incubated for 45 min and initiated with ADP at a final concentration of 0.5 mM.

IIA^{glc} Inhibition of Wildtype and E36C. To characterize the extent of IIA^{glc} inhibition of E36C compared to wildtype, inhibition studies were performed for both enzymes. Activity was analyzed as a function of IIA^{glc} concentration for both enzymes and the results are shown in Figures 11 and 12. The fits were generated using Equation

4, which provided the parameter $K_{0.5}$. The parameter W was determined using Equation 2. The results are compared in the table on page 40.

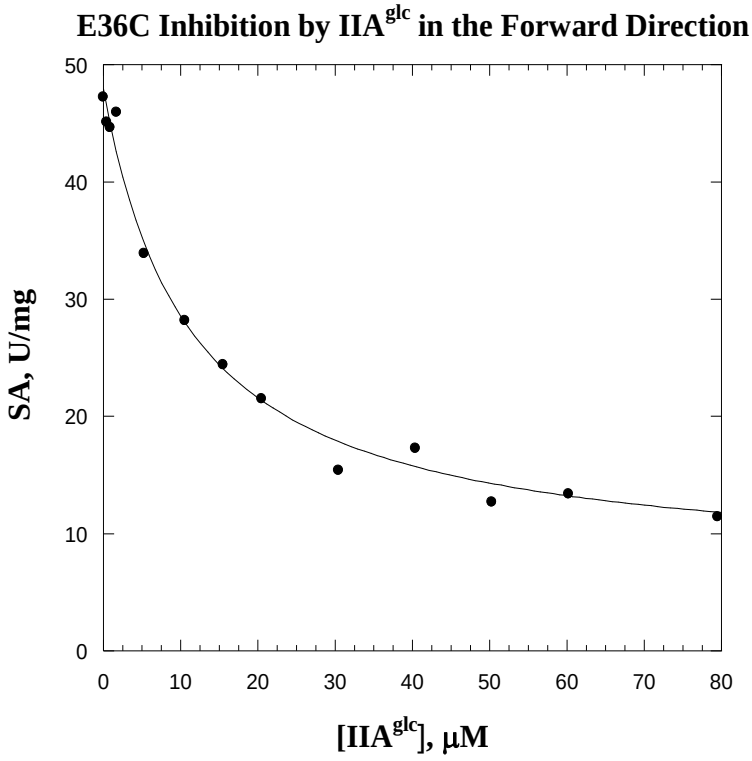

Figure 11: E36C Inhibition by IIA^{glc} in the Forward Direction. Each point on the graph indicates an individual assay conducted at the indicated IIA^{glc} concentration. The line shows the fit to Equation 4. W was obtained using Equation 2. Each assay was initiated with E36C at a final concentration of 0.5 μg/mL.

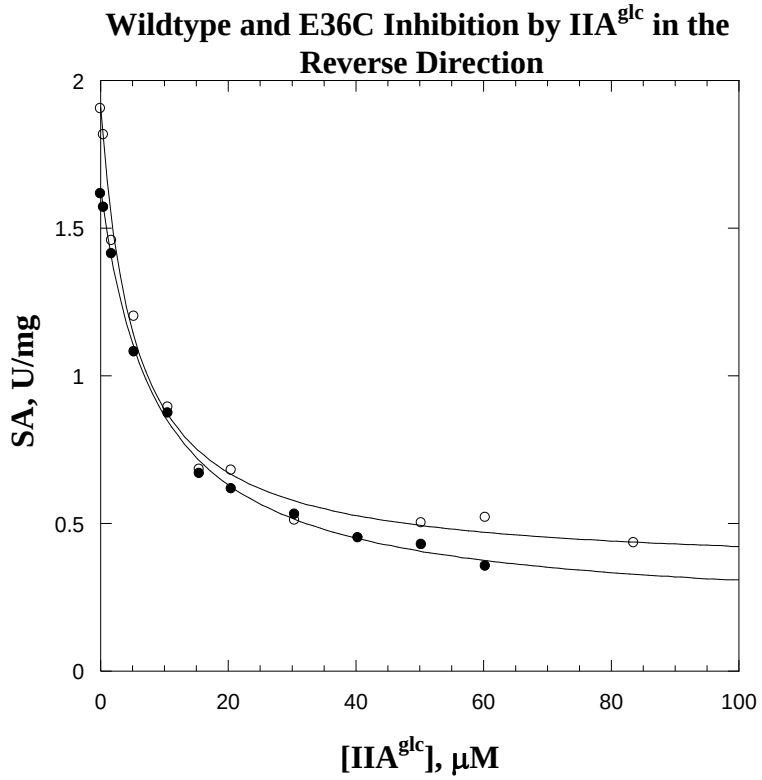

Figure 12: Wildtype and E36C Inhibition by IIA^{glc} in the Reverse Direction. Each point on the graph indicates an individual assay conducted at the indicated IIA^{glc} concentration. The open circles represent wildtype and the filled circles represent E36C. The line shows the fit to Equation 4. W was obtained using Equation 2. Each assay was initiated with EcGK at a final concentration of 8.5 μg/mL.

Heterotropic Coupling Between FBP and ATP/ADP. Heterotropic coupling assays were performed to see if binding of either of the nucleotides influences binding of FBP. To analyze this question, assays were performed where ATP or ADP were varied at different fixed concentrations of FBP. The fits of the assays that contained ATP are shown in Figures 13 and 14. The solid lines in these figures represent the best fit from using Equation 6. The parameters are compared in the table on page 40.

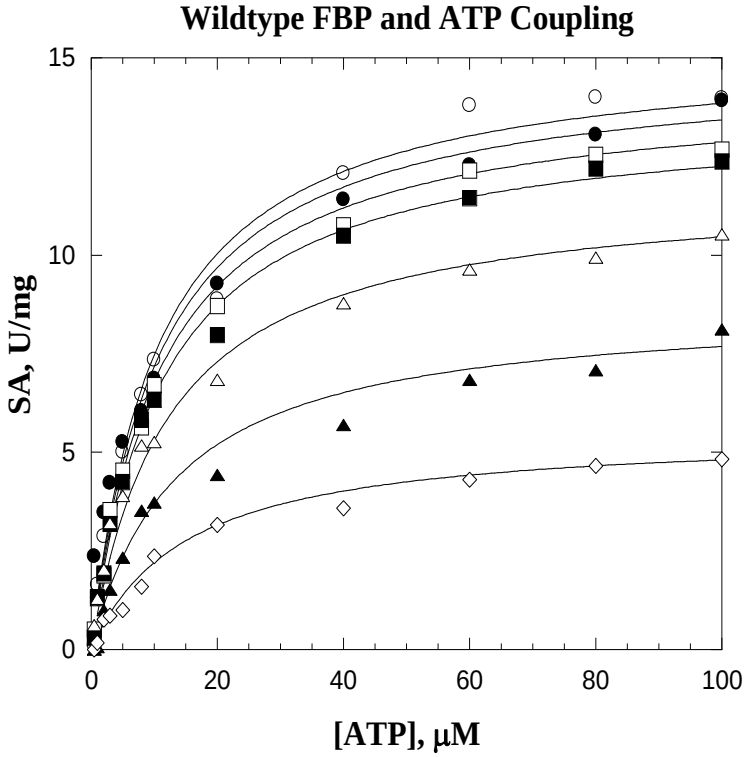

Figure 13: Wildtype FBP and ATP Coupling. Each point on the graph indicates an individual assay conducted at the indicated ATP concentration. The concentration of FBP is 0 μM for the top curve represented by the open circles. Each curve underneath increases in concentration: 15 μM, 30 μM, 45 μM, 91 μM, 185 μM, and 350 μM FBP. The lines show the fits to Equation 6. Each assay was incubated for 45 min and initiated with the indicated concentration of ATP.

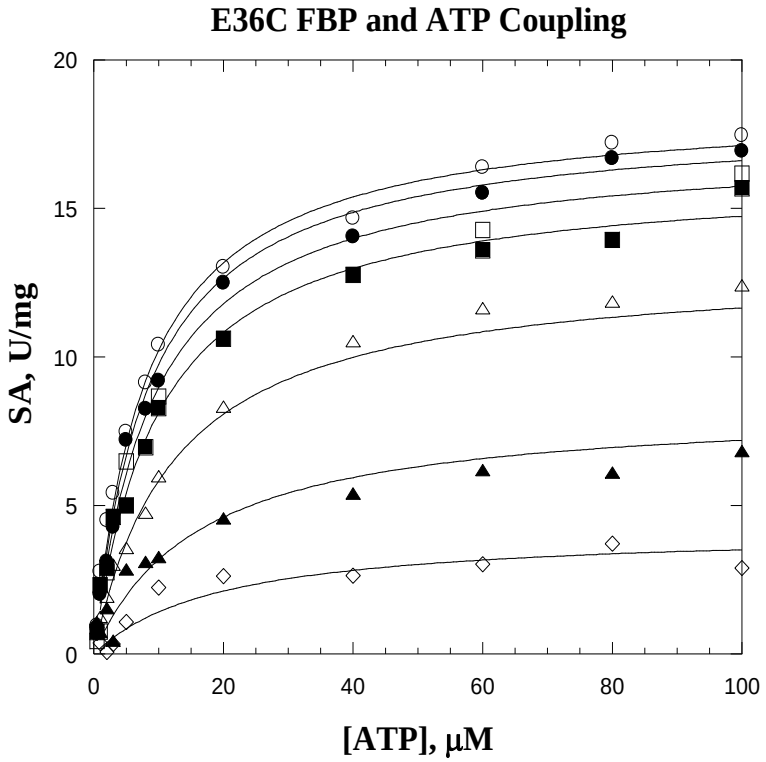

Figure 14: E36C FBP and ATP Coupling. Each point on the graph indicates an individual assay conducted at the indicated ATP concentration. The concentration of FBP is 0 μM for the top curve and is represented by the open circles. Each curve underneath increases in concentration: 15 μM, 30 μM, 45 μM, 91 μM, 185 μM, and 350 μM FBP. The lines show the fits to Equation 6. Each assay was incubated for 45 min and initiated with the indicated concentration of ATP.

The fits of the assays that contained ADP are shown in Figures 15 and 16. The solid lines in these figures represent the best fit from using Equation 6.

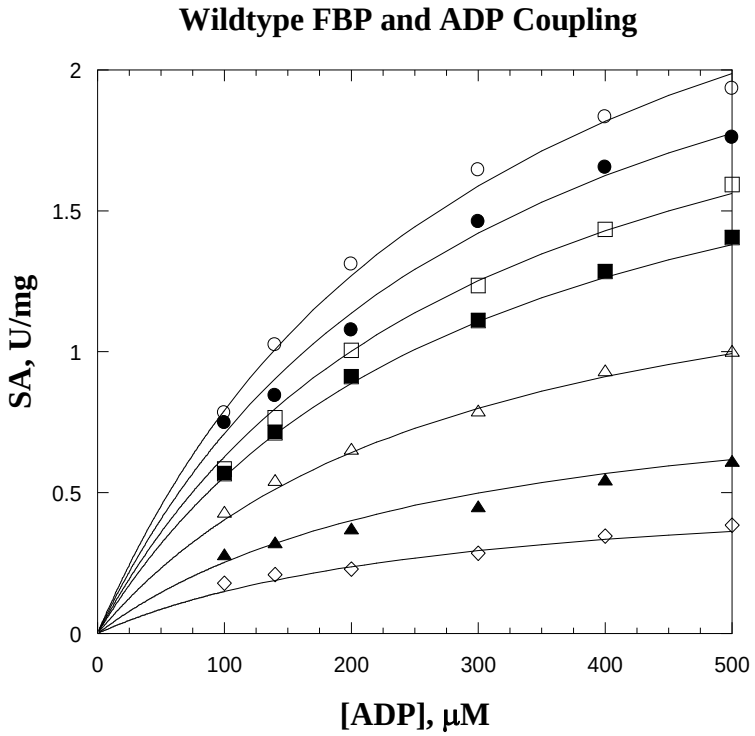

Figure 15: Wildtype FBP and ADP Coupling. Each point on the graph indicates an individual assay conducted at the indicated ADP concentration. The concentration of FBP is 0 μM for the top curve represented by the open circles. Each curve underneath increases in concentration: 15 μM, 30 μM, 45 μM, 91 μM, 185 μM, and 350 μM FBP. The lines show the fits to Equation 6. Each assay was incubated for 45 min and initiated with the indicated concentration of ADP.

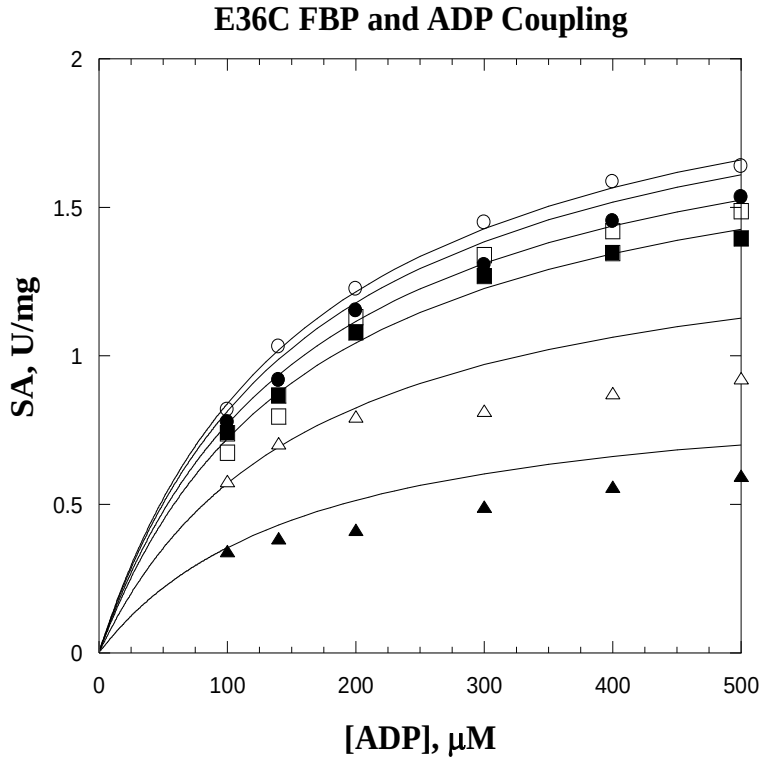

Figure 16: E36C FBP and ADP Coupling. Each point on the graph indicates an individual assay conducted at the indicated ADP concentration. The concentration of FBP is 0 μM for the top curve represented by the open circles. Each curve underneath increases in concentration: 15 μM, 30 μM, 45 μM, 91 μM, and 185 μM FBP. The lines show the fits to Equation 6. Each assay was incubated for 45 min and initiated with the indicated concentration of ADP.

Heterotropic Coupling Between IIA^{glc} and ATP/ADP. Heterotropic coupling assays were performed to see if binding of either of the nucleotides influence inhibition by IIA^{glc}. As with FBP, the assays were performed with varied ATP or ADP concentrations at different fixed concentrations of IIA^{glc}. The fits of the data are shown in Figures 17-19. The solid lines in these figures represent the best fit from using Equation 7 and the extracted parameters are summarized in the table on page 40.

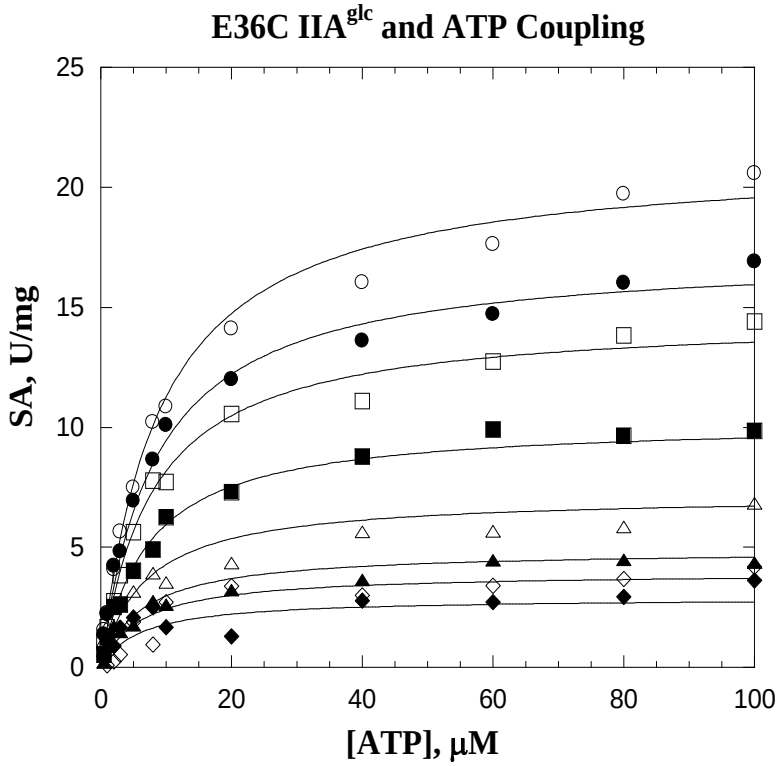

Figure 17: E36C IIA^{glc} and ATP Coupling. Each point on the graph indicates an individual assay conducted at the indicated ATP concentration. The concentration of IIA^{glc} is 0 μM for the top curve represented by the open circles. Each curve underneath increases in concentration: 1 μM, 2 μM, 5 μM, 10 μM, 20 μM, 30 μM, and 60 μM IIA^{glc}. The lines show the fits to Equation 7. Each assay was initiated with the EcGK at a final concentration of 0.5 μg/mL.

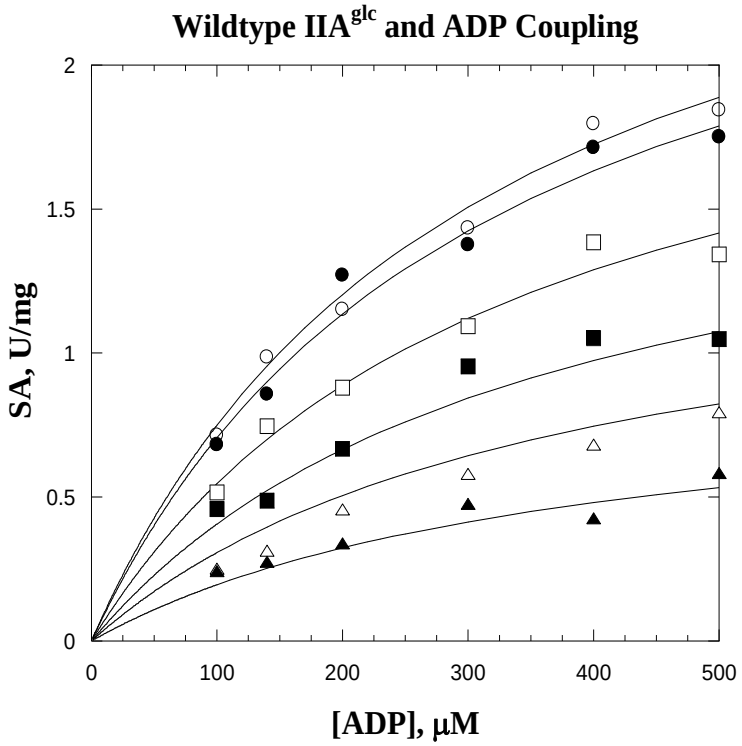

Figure 18: Wildtype IIA^{glc} and ADP Coupling. Each point on the graph indicates an individual assay conducted at the indicated ADP concentration. The concentration of IIA^{glc} is 0 μM for the top curve represented by the open circles. Each curve underneath increases in concentration: 1 μM, 5 μM, 10 μM, 20 μM, and 40 μM IIA^{glc}. The lines show the fits to Equation 7. Each assay was initiated with the EcGK at a final concentration of 8.5 μg/mL.

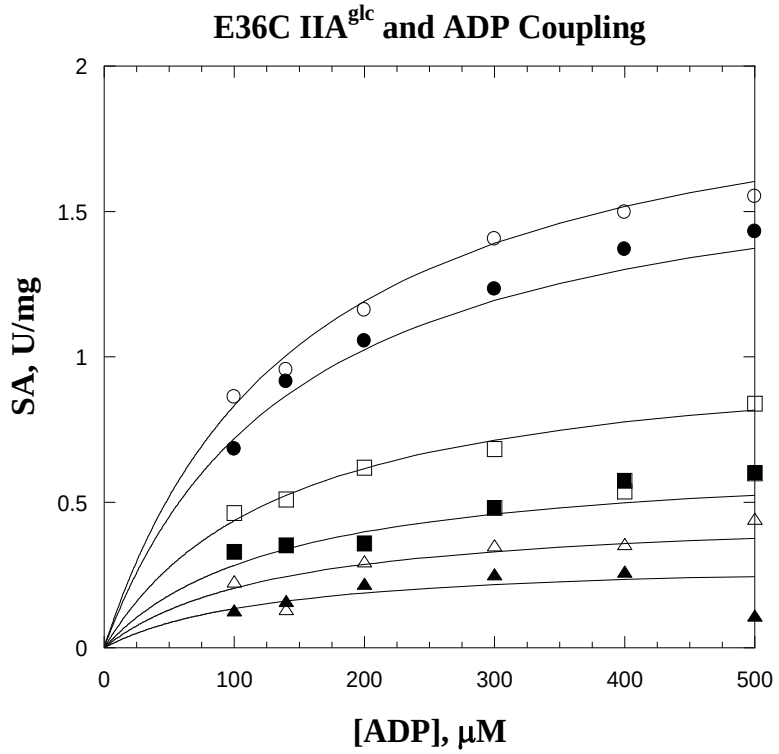

Figure 19: E36C IIA^{glc} and ADP Coupling. Each point on the graph indicates an individual assay conducted at the indicated ADP concentration. The concentration of IIA^{glc} is 0 μM for the top curve represented by the open circles. Each curve underneath increases in concentration: 1 μM, 5 μM, 10 μM, 20 μM, and 40 μM IIA^{glc}. The lines show the fits to Equation 7. Each assay was initiated with the EcGK at a final concentration of 8.5 μg/mL.

All the parameters extracted from initial velocity, inhibition, and heterotropic coupling studies shown above are summarized in Table 1. The wildtype K_m for glycerol was taken from previously published data for comparison (5). The results of E36C inhibition by IIA^{glc} in the forward reaction were compared to the published results for wildtype inhibition by IIA^{glc} (5) Those of the reverse reaction for both enzymes during the IIA^{glc} inhibition studies were compared independently in this work.

Table 1: E36C Substitution Effects on EcGK Activity

	FORWARD		REVERSE	
PARAMETER	**WILDTYPE**	**E36C**	**WILDTYPE**	**E36C**
	Initial Velocity Studies			
V_{max} U/mg	50 ± 1[b]	56 ± 2	2.0 ± 0.2	1.5 ± 0.1
$K_m^{Gol/G3P}$, µM	37 ± 4[b]	27.2 ± 4.4	305 ± 60	246 ± 36
	FBP Inhibition Studies			
SA_0 U/mg	41 ± 2[a]	49 ± 1	1.9 ± 0.1	1.8 ± 0.1
$K_{0.5}$, FBP (µM)	630 ± 90[a]	478 ± 17	97 ± 4	120 ± 5
W_{FBP}	0.02 ± 0.05[a]	0.06 ± 0.01	0.05 ± 0.01	0.11 ± 0.02
n_H	1.6 ± 0.3[a]	1.7 ± 0.1	1.3 ± 0.1	1.6 ± 0.1
	IIA^{glc} Inhibition Studies			
SA_0 U/mg	36 ± 1[a]	48 ± 1	1.9 ± 0.1	1.6 ± 0.1
$K_{0.5}$, IIA^{glc} (µM)	6.3 ± 1.0[a]	11 ± 2	5 ± 1	9 ± 1
W_{IIAglc}	0.07 ± 0.04[a]	0.14 ± 0.07	0.16 ± 0.01	0.13 ± 0.05
	FBP and ATP/ADP Heterotropic Coupling			
V_{max} U/mg	15 ± 1	19 ± 1	3.2 ± 0.1	2.2 ± 0.1
$K_m^{ATP/ADP}$, µM	11 ± 1	8 ± 1	304 ± 17	162 ± 1
$K_{0.5}$, FBP (µM)	149 ± 29	82 ± 1	89 ± 10	148 ± 2
W_{FBP}	0.03 ± 0.13	0.01 ± 0.01	0.04 ± 0.03	0.01 ± 0.01
Q_{FBP}	0.6 ± 0.2	0.4 ± 0.1	1.1 ± 0.2	0.8 ± 0.1
n_H	1.3 ± 0.2	1.5 ± 0.1	1.2 ± 0.1	1.1 ± 0.1
	IIA^{glc} ATP/ADP Heterotropic Coupling			
V_{max} U/mg	21 ± 1[a]	21 ± 1	3.1 ± 0.2	2.1 ± 0.1
$K_m^{ATP/ADP}$, µM	12 ± 2[a]	8.9 ± 0.5	307 ± 38	151 ± 23
$K_{0.5}$, IIA^{glc} (µM)	7 ± 2[a]	5.8 ± 1.0	13 ± 4	5.6 ± 2.1
W_{IIAglc}	0.03 ± 0.02[a]	0.08 ± 0.01	0.001 ± 0.07	0.05 ± 0.03
Q_{IIAglc}	1.6 ± 0.6[a]	1.5 ± 0.3	0.74 ± 0.37	1.2 ± 0.6

a: Values taken from Pettigrew (5)
b: Values taken from Acquaye (24)

This table compares the parameters for both wildtype and E36C in both the "forward" and "reverse" directions. The forward direction involves going from ATP/Gol to ADP/G3P and the revere involves going from ADP/G3P to ATP/Gol. The K_m values for the substrates are listed in the left foremost column as $K_m^{Gol/G3P}$ and $K_m^{ATP/ADP}$. If the corresponding value is under the "forward" subheading, the value corresponds to Gol or ATP and if under the "reverse" subheading it corresponds to G3P or ADP. The values are reported with their standard errors.

The V_{max} values for all of the experiments were similar for both wildtype and E36C and the initial velocity studies for determining the K_m^{Gol} and K_m^{G3P} for both wildtype and E36C yielded similar results for the K_m values. Comparing FBP and IIA^{glc} inhibition produced small differences between the two enzymes. The W_{FBP} in the reverse direction was 2-fold higher for E36C than wildtype and the $K_{0.5}^{IIAglc}$ in the reverse direction is 2-fold higher for E36C. From the FBP and ATP heterotropic coupling experiments, the $K_{0.5}^{FBP}$ is 2-fold less than wildtype for E36C. The FBP and ADP heterotropic coupling, however, has a 2-fold higher $K_{0.5}^{FBP}$ and 2-fold lower K_m^{ADP} for E36C compared to wildtype. The only difference between the two enzymes from the IIA^{glc} heterotropic coupling assays is that the K_m^{ADP} is 2-fold less for E36C than wildtype.

6IAF Labeling Effects on FBP and IIA^{glc} Inhibition. The effect of labeling E36C was tested by four different mixtures: untreated, time zero, labeled E (excess), and labeled C (clean). The untreated sample is E36C incubated with 10 mM DTT, purified on the NAP-10 column, tested for concentration, and had the ATP addition. The time zero point was a sample of E36C that was incubated for 30 min in Sephacryl buffer with 10 mM DTT, purified on the NAP-10 column, tested for concentration, and had the ATP addition. The key difference was that 10 μL of 1:10 β-Me was added to the sample before 6IAF, thus preventing labeling and creating a time zero sample (which contains quenched 6IAF). The labeled E was a sample that went through all the conventional steps and waited for 15 min of labeling before adding the β-Me. This sample, however, was not cleaned on the NAP-10 column or dialyzed after labeling and therefore

contained the excess β-Me, ATP, and quenched 6IAF. The labeled C sample went through all conventional steps, including the NAP-10 column and dialysis after labeling, removing excess quenched 6IAF. Each sample was tested for their FBP (Figure 20) and IIA^{glc} (Figure 21) inhibition as described in the Materials and Methods section. The concentration of the inhibitor was varied as shown in the figures and the results summarized in Table 2.

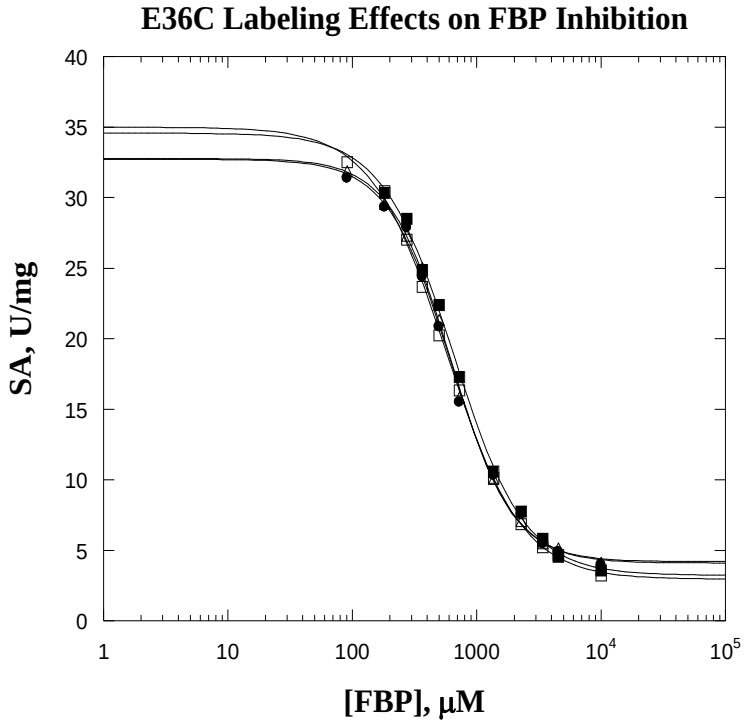

Figure 20: E36C Labeling Effects on FBP Inhibition. Each point on the graph indicates an individual assay conducted at the indicated concentration of FBP. The filled circles represent "untreated", open squares represent "time zero", filled squares represent "labeled E", and open triangles represent "labeled C". The lines show the fits to Equation 5 and the parameters extracted from these fits are presented in Table 2 below. Each assay was incubated for 45 min and initiated with ATP at a final concentration of 2.5 mM.

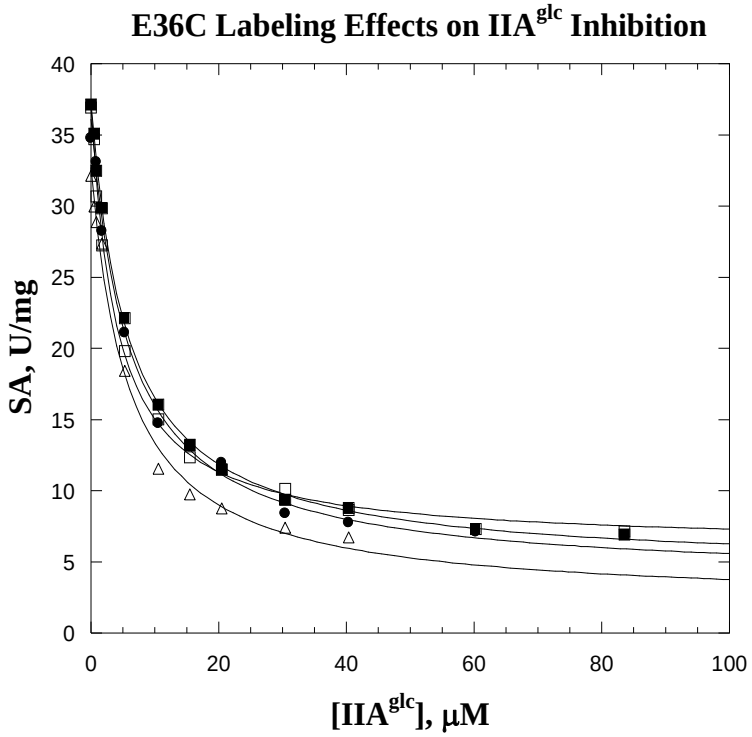

Figure 21: E36C Labeling Effects on IIA^{glc} Inhibition. Each point on the graph indicates an individual assay conducted at the indicated concentration of IIA^{glc}. The filled circles represent "untreated", open squares represent "time zero", filled squares represent "labeled E", and open triangles represent "labeled C". The lines show the fits to Equation 5 and the parameters extracted from these fits are presented in Table 2 below. Each assay was initiated with EcGK at a final concentration of 0.5 μg/mL.

Table 2: 6IAF Labeling Effects on FBP and IIA^{glc} Inhibition

	FBP Inhibition			
ENZYME PREP	**SA_0, U/mg**	**$K_{0.5}$, μM**	**W**	**n_H**
Untreated	33 ± 1	617 ± 29	0.13 ± 0.02	1.7 ± 0.1
Time Zero	35 ± 1	574 ± 19	0.08 ± 0.01	1.4 ± 0.1
Labeled E	35 ± 1	650 ± 42	0.09 ± 0.02	1.5 ± 0.1
Labeled C	33 ± 1	620 ± 16	0.13 ± 0.01	1.8 ± 0.1
	IIA^{glc} Inhibition			
ENZYME	**SA_0, U/mg**	**$K_{0.5}$, μM**	**W**	**n_H**
Untreated	36 ± 1	6.1 ± 0.8	0.10 ± 0.03	NA
Time Zero	37 ± 1	4.1 ± 0.3	0.16 ± 0.01	NA
Labeled E	37 ± 1	5.8 ± 0.2	0.12 ± 0.01	NA
Labeled C	33 ± 1	5.8 ± 1.0	0.10 ± 0.01	NA

These results are from a non-linear least squares fitting of the inhibition data using Equations 2 and 3. This was done with the Kaleidagraph software from Synergy. The parameter W describes the extent of inhibition by IIA^{glc} and is obtained from Equation 2. All of these assays were performed in the "forward" direction. NA is not applicable. Values are given with standard errors.

Although there does exist some slight variation between the treatments, the differences are small. For FBP inhibition, all of the specific activities are comparable, as well as the $K_{0.5}$, W, and n_H values. For IIA^{glc} inhibition, the parameters are again comparable between the different treatments. The largest difference observed is for the time zero sample but, due to the closeness of the parameters, it is not statistically different from untreated, labeled E, or labeled C.

6IAF Time Course Study. To evaluate whether the specific activity of the enzyme changes during the labeling process, a time course experiment was conducted and the results are shown below in Figure 22. For this experiment, the sample went through all the conventional steps up to adding the 6IAF. Once labeling was initiated with 6IAF, aliquots were removed and quenched with 1 μL of 1:10 β-Me at the time

points indicated in the figure. The assays were composed of the forward cocktail, 2.5 mM ATP, and 10 mM glycerol.

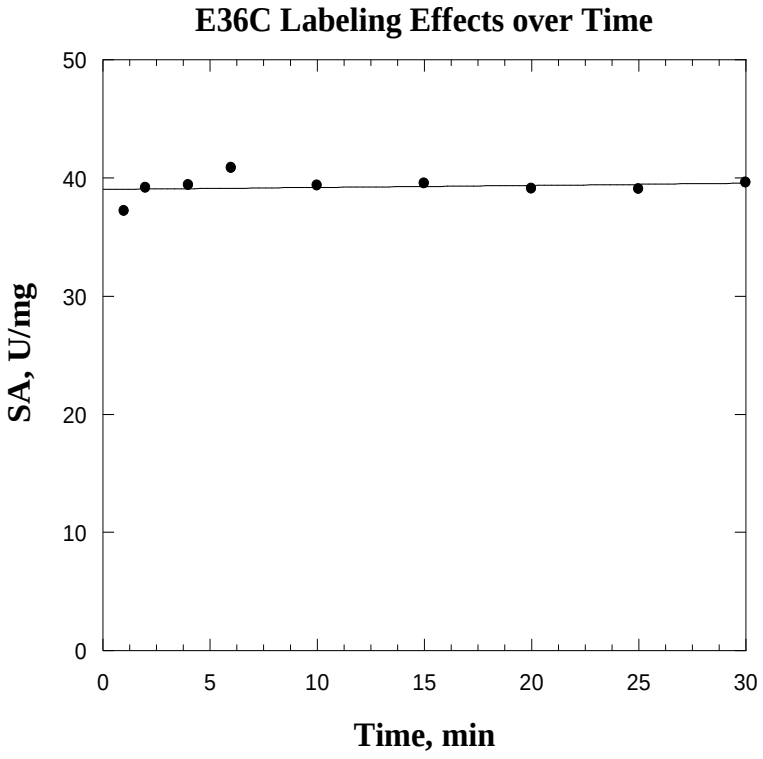

Figure 22: E36C Labeling Effects over Time. Each point on the graph indicates an individual assay conducted at the indicated time to determine if specific activity changes during the labeling process. The slope is 0.01 U $mg^{-1}min^{-1}$ and the V_{max} is 39.0 ± 0.5. Each assay was initiated with EcGK at a final concentration of 0.5 µg/mL.

The pattern of activity in Figure 22 shows a slight increase in activity that returns to normal levels over time. The slope generated from the plot 0.01 U mg^{-1} min^{-1} and is not significant enough to establish an effect of 6IAF on enzyme activity during the labeling process.

Defining the Effect of Ligand Binding on the Fluorescence Properties of 6IAF Labeled E36C

Effects of Ligand Binding on Fluorescence. To determine whether the fluorescence properties of the extrinsic fluorophore are altered by ligand binding, a variety of ligand combinations were tested. Only labeled E36C with a stoichiometry of 0.12 (mol of fluorescein / mol EcGK subunit) or less was used and added to a final concentration of 250 nM (subunits). This low stoichiometry was used since higher stoichiometries above 0.12 resulted in Homo-FRET. When ATP or ADP was part of the complex being tested, the final concentration was 5 mM. When glycerol or G3P were part of the complex, the final concentration was 2 mM.

To assess the possibility of Q-coupling, all complexes were tested in the absence and presence of the effectors IIA^{glc} and FBP. When these effectors were added, IIA^{glc} was added to a final concentration of 80 μM and FBP was added to a final concentration of 8mM. Volumes were made up to 1.4 mL for each assay using 0.1 M TEA pH 7.0 and allowed to warm up in the spectrophotometer for 5 min, 15 min for samples that contained FBP to allow tetramer formation. All anisotropy values were calculated by the Vinci Software program. The tested complexes and their results are recorded in Table 3. Although both anisotropy and intensity data were recorded, intensity changes were less than 10% and thus only anisotropy was considered useful for comparison.

Table 3: Effects of Ligand Binding on E36C:6IAF Anisotropy

	ALLOSTERIC EFFECTOR		
LIGANDS	**NONE**	**FBP**	**IIA^{glc}**
	ANISOTROPY	**ANISOTROPY**	**ANISOTROPY**
None	0.158 ± 0.004 (4)	0.157 ± 0.002 (3)	0.167 ± 0.002 (2)
ATP	0.167 ± 0.003 (3)	0.166 ± 0.001 (2)	0.189 ± 0.001 (1)
Glycerol	0.173 ± 0.005 (3)	0.163 ± 0.001 (2)	0.171 ± 0.001 (1)
ATP/Glycerol	0.200 ± 0.011 (3)	0.164 ± 0.010 (3)	0.174 ± 0.009 (3)
ADP	0.181 ± 0.003 (3)	0.178 ± 0.004 (2)	0.187 ± 0.004 (2)
G3P	0.173 ± 0.002 (3)	0.166 ± 0.003 (2)	0.170 ± 0.002 (2)
ADP/G3P	0.186 ± 0.006 (3)	0.166 ± 0.009 (3)	0.179 ± 0.009 (3)

Anisotropy values are given as the mean ± standard deviation for the number of trials shown in parenthesis. When the number of trials is 2, the uncertainty is propagated from the relative uncertainties of the individual values. When the number of trials is 1, the uncertainty is the value for the individual determination as given by the Vinci software.

According to the anisotropy values, all substrates increase the anisotropy when compared to the enzyme alone by at least 0.009 and the highest increase in anisotropy occurs when both ATP and glycerol or ADP and G3P are bound. FBP addition to each of the complexes tested shows that FBP decreases the anisotropy of the enzyme/ATP/Gol and enzyme/ADP/G3P ternary complexes. IIA^{glc} addition increases the anisotropy of the enzyme/ATP and enzyme/ATP/Gol complexes.

Titration of the Ternary Complexes with Allosteric Effectors. By analyzing how the allosteric effectors FBP and IIA^{glc} change the anisotropy of the ternary complexes, the $K_{0.5}$ can be determined. These values can then be compared to those observed from the kinetics assay performed previously.

Titrations of the EAB (enzyme/ATP/glycerol) and EPQ (enzyme/ADP/G3P) complexes were performed to determine the $K_{0.5}$ for FBP and IIA^{glc}. Each 1.4 mL assay contained 250 nM subunits of the enzyme and 0.1 M TEA pH 7.0. All samples were incubated in the spectrophotometer for 5 min unless they contained FBP, then they incubated for 15 min. The assays involving the EAB complex contained 2 mM glycerol and either 2.5 mM ATP or 100 μM ATP. Two different concentrations of ATP were used because EcGK has two apparent binding sites for ATP. The first is saturated at 100 μM ATP and the second is saturated at 2.5 mM ATP. The titrant in each case was the inhibitor and it was varied as shown in the figures. One trial of each titration is shown as a representative of the assay in Figures 23 and 25 for the EAB complex.

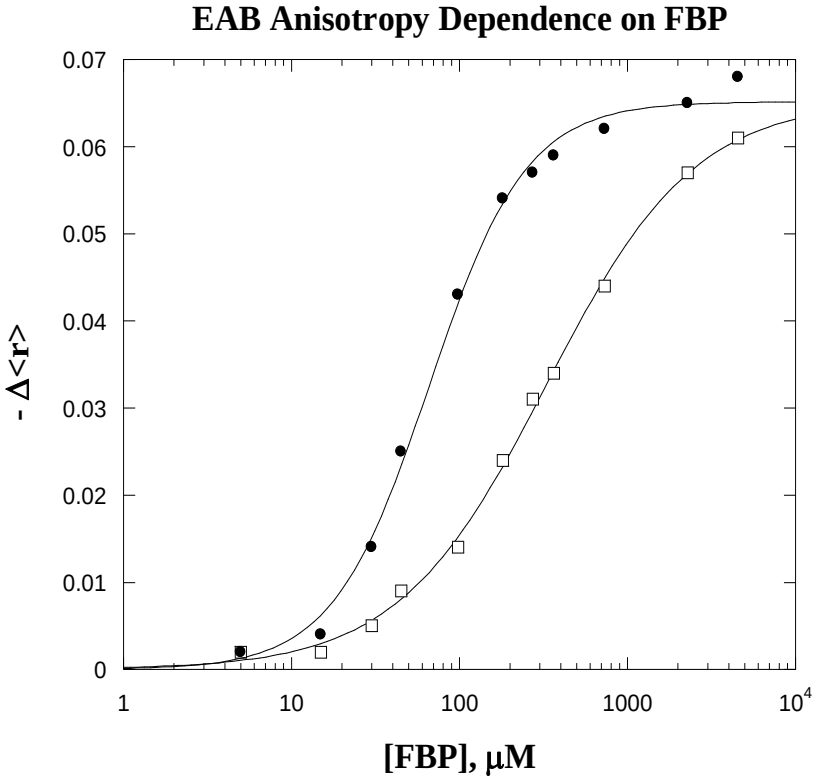

Figure 23: EAB Anisotropy Dependence on FBP. EAB is the enzyme/ATP/glycerol complex. Each point on the graph indicates an individual assay conducted at the indicated FBP concentration. The filled circles represent assays performed at 100 μM ATP and the open squares represent those performed at 2.5 mM ATP. The data are graphed as a change in anisotropy (Δ<r>) between X μM of FBP and 0 μM of FBP for the ternary complex. The lines show the fits to Equation 8.

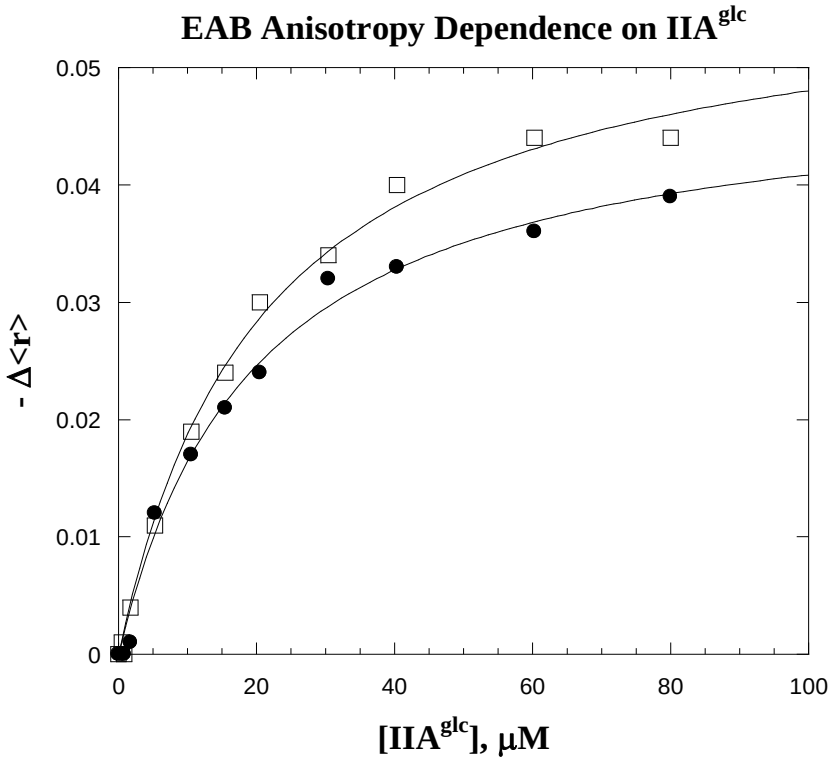

Figure 24: EAB Anisotropy Dependence on IIA^{glc}. EAB is the enzyme/ATP/glycerol complex. Each point on the graph indicates an individual assay conducted at the indicated IIA^{glc} concentration. The filled circles represent assays performed at 100 μM ATP and the open squares represent those performed at 2.5 mM ATP. The data are graphed as a change in anisotropy (Δ<r>) between X μM of IIA^{glc} and 0 μM of IIA^{glc} for the ternary complex. The lines show the fits to Equation 8.

When testing the EPQ complex, the assays contained 2 mM G3P and 2.5 mM ADP. The titrant in each case was again the inhibitor and it was varied as shown in the figures. One trial of each titration is shown as a representative of the assay in Figures 25 and 26.

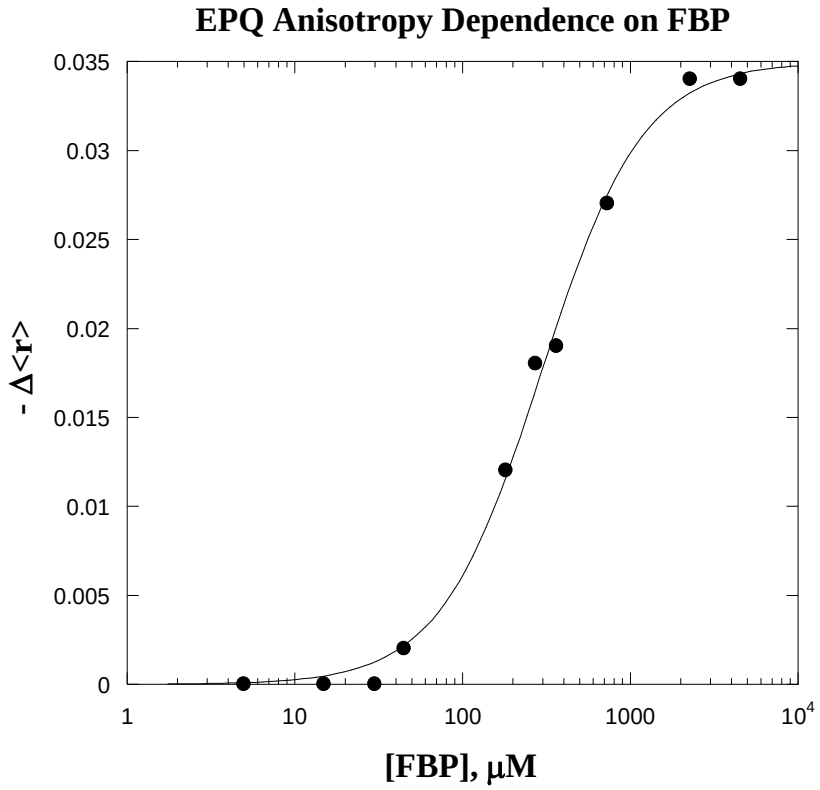

Figure 25: EPQ Anisotropy Dependence on FBP. EPQ is the enzyme/ADP/G3P complex. Each point on the graph indicates an individual assay conducted at the indicated FBP concentration and at 2.5 mM ADP. The data is graphed as a change in anisotropy (Δ<r>) between X μM of FBP and 0 μM of FBP for the ternary complex. The lines show the fits to Equation 8.

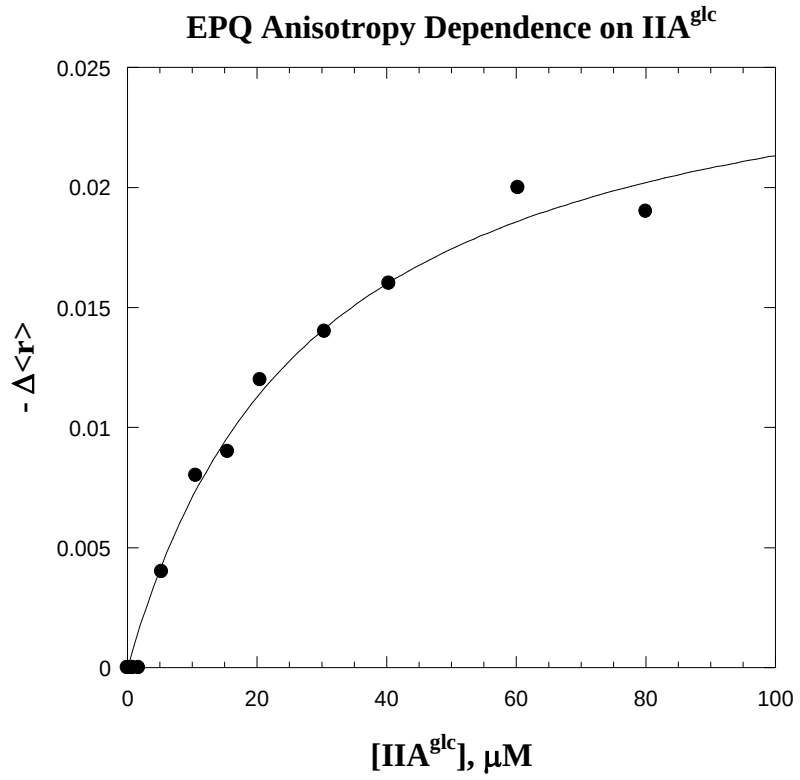

Figure 26: EPQ Anisotropy Dependence on IIA^{glc}. EPQ is the enzyme/ADP/G3P complex. Each point on the graph indicates an individual assay conducted at the indicated IIA^{glc} concentration and at 2.5 mM ADP. The data is graphed as a change in anisotropy ($\Delta\langle r\rangle$) between X μM of IIA^{glc} and 0 μM of IIA^{glc} for the ternary complex. The lines show the fits to Equation 8.

The results for $K_{0.5}$ and n_H (for FBP) are averaged from two trials and summarized in Table 4 for both the EAB and EPQ complexes. Table 4 also summarizes the parameters extracted for both complexes in the presence and absence of IIA^{glc}.

Table 4: EAB and EPQ Anisotropy Dependence on Allosteric Effectors FBP and IIA^{glc}

	EAB COMPLEX			EPQ COMPLEX		
TITRANT	**-Δ<r> max**	**$K_{0.5}$**	**n_H**	**-Δ<r> max**	**$K_{0.5}$**	**n_H**
FBP 2.5mM ATP/ADP	0.068 ± 0.001	346 ± 15	0.9 ± 0.1	0.032 ± 0.001	269 ± 10	1.5 ± 0.1
FBP 100µM ATP	0.064 ± 0.001	67 ± 3	1.5 ± 0.1			
IIA^{glc} 2.5mM ATP/ADP	0.058 ± 0.001	23 ± 1	NA	0.033 ± 0.002	36±4	NA
IIA^{glc} 100µM ATP	0.053 ± 0.002	21 ± 3	NA			

(EAB=Enzyme/ATP/Glycerol, EPQ=Enzyme/ADP/G3P). All values presented in this table are averages from two independent experiments and are reported with propagated uncertainty. The errors are propagated from the two trials. The shaded boxes indicate that no experiments were performed to assess the effects at 100µM ADP when analyzing the EPQ complex. NA is not applicable.

$K_{0.5}$ values for FBP and IIA^{glc} were able to be extracted from the fluorescence titrations. For the FBP titrations, the $K_{0.5}$ and n_H values were attainable for both ATP concentrations tested and for ADP. The $K_{0.5}^{FBP}$ value at 2.5 mM ATP was 3-fold higher than the value at 100 µM ATP. The n_H value for 2.5mM ATP was 0.9 and that for 100µM ATP was 1.5 indicating a difference in FBP homotropic interactions at the different ATP concentrations.

Evaluating the Potential Use of EcGK Native Cysteines as Probes for Ligand Induced Conformational Changes

Cysteine Substitution Effects on EcGK Activity. The five cysteine mutants analyzed were C292S, C255S, C269A, C105S:C112A, and C105S:C112V. The three single cysteine mutants were analyzed after completing the third column purification

step (Source 15Q pH 8.0). The dual cysteine mutants were purified and analyzed by Mr. Frank N. Raushel as a crude extract after the ammonium sulfate treatment.

Each single substitution was tested for its effect on the catalytic and allosteric parameters of EcGK. The dual cysteine substitutions were only tested for effects on inhibition. Both the initial velocity assays and IIA^{glc} inhibition assays were initiated with EcGK to a final concentration of 0.5 μg/mL for C292S, 1 μg/mL for C255S and C269A, and by addition of 50 μL of ammonium sulfate treated cell lysate for C105S:C112A and C105S:C112V. All assays were performed at 25 ^{o}C and pH 7.0 using the forward cocktail. ATP, glycerol, IIA^{glc}, and FBP were all varied as shown in the figures. The effect on glycerol and ATP dependence for the single substitutions (C292S, C255S, and C269A) are shown in Figure 27 and Figure 28, respectively. The data were fit to Equation 1 using Kaleidagraph Synergy software.

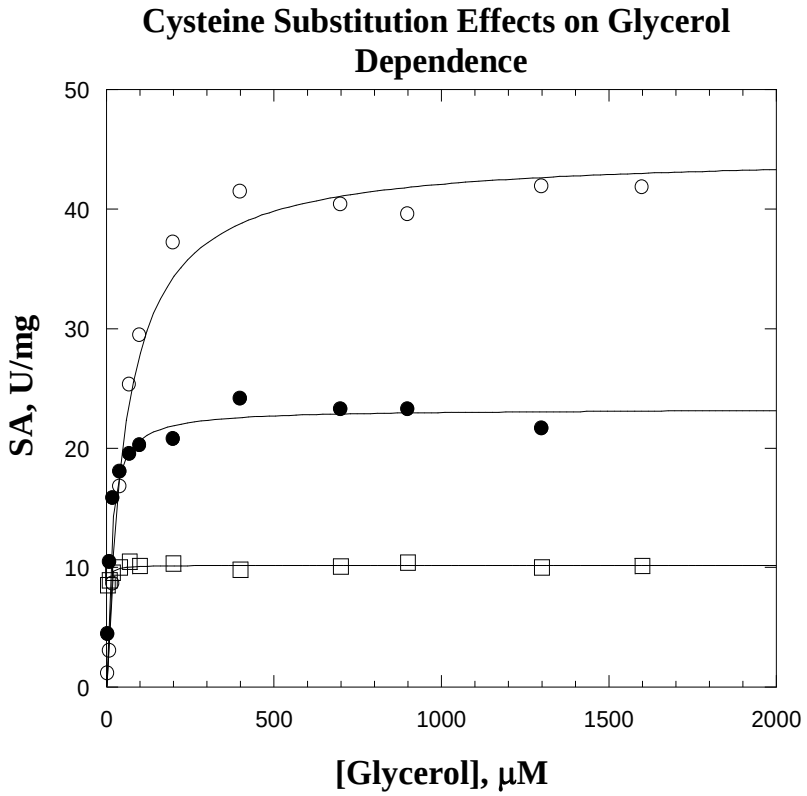

Figure 27: Cysteine Substitution Effects on Glycerol Dependence. Each point on the graph indicates an individual assay conducted at the indicated glycerol concentration and was initiated by the addition of EcGK to a final concentration as described previously. The open circles represent C292S, the filled circles represent C255S, and the open squares represent C269A. The lines show the fits to Equation 1.

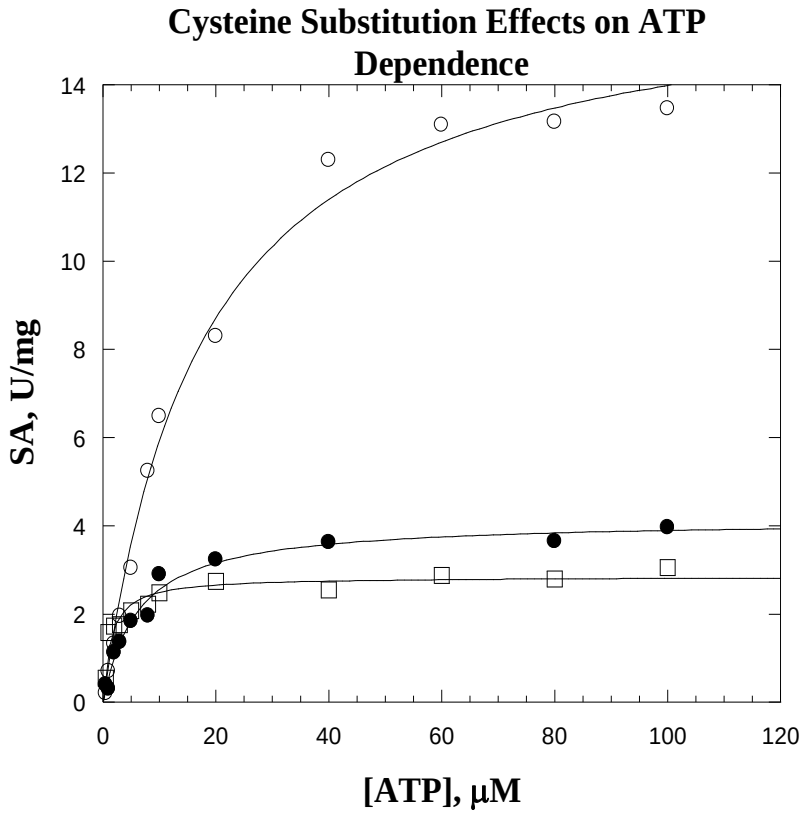

Figure 28: Cysteine Substitution Effects on ATP Dependence. Each point on the graph indicates an individual assay conducted at the indicated ATP concentration and was initiated by the addition of EcGK to a final concentration as described previously. The open circles represent C292S, the filled circles represent C255S, and the open squares represent C269A. The lines show the fits to Equation 1.

The effect of the single cysteine substitutions on FBP inhibition are in Figure 29 for C292S, and Figure 30 for C255S and C269A. The fits were generated using Equation 4 with Kaleidagraph Synergy Software.

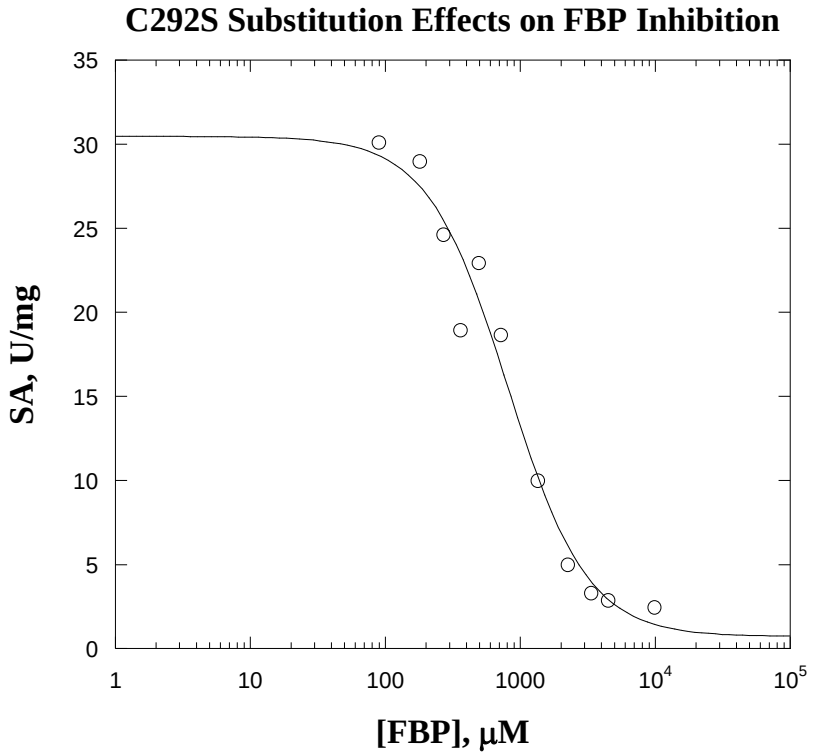

Figure 29: C292S Substitution Effects on FBP Inhibition. Each point on the graph indicates an individual assay conducted at the indicated FBP concentration. Each assay was incubated for 45 min with EcGK and initiated by the addition of ATP to a final concentration of 2.5 mM. The lines show the fits to Equation 4.

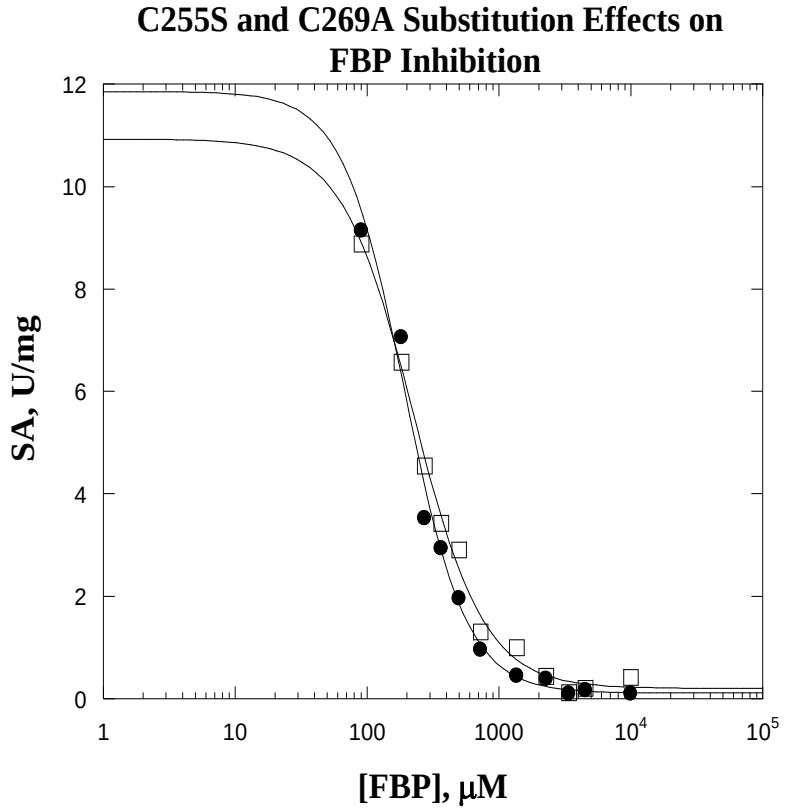

Figure 30: C255S and C269A Substitution Effects on FBP Inhibition. Each point on the graph indicates an individual assay conducted at the indicated FBP concentration. Each assay was incubated for 45 min with EcGK and initiated by the addition of ATP to a final concentration of 2.5 mM. The open circles represent C255S and the filled circles represent C269A. The lines show the fits to Equation 4.

Figures 31 and 32 show the dual cysteine substitution effect on FBP inhibition for C105S:C112A and C105S:C112V, respectively. This fits were generated using Kaleidagraph and Equation 4.

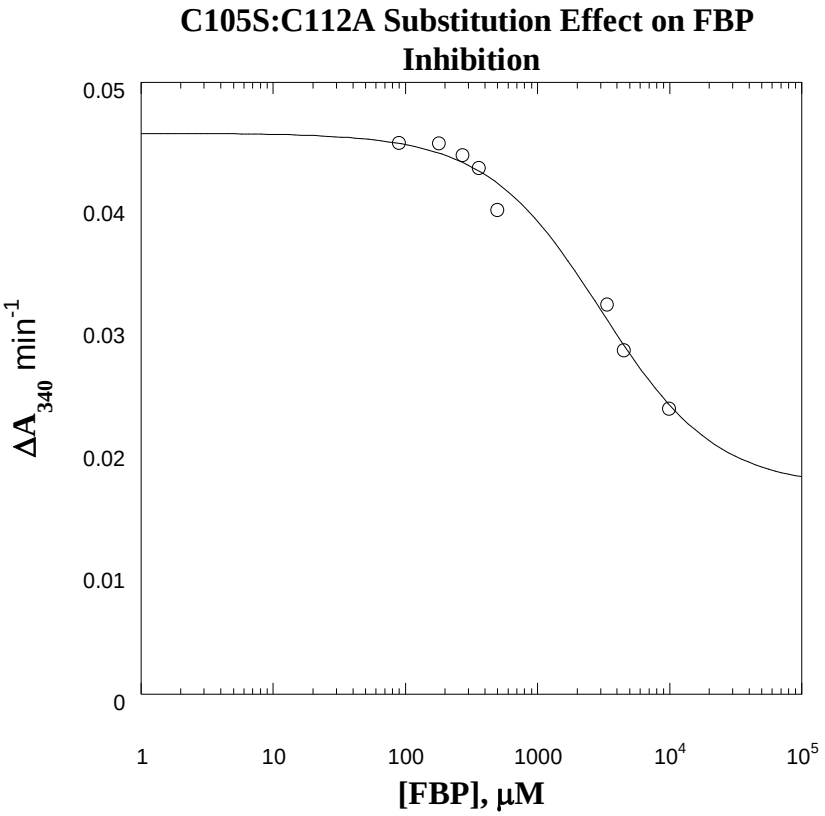

Figure 31: C105S:C112A Substitution Effect on FBP Inhibition . Each point on the graph indicates an individual assay conducted at the indicated FBP concentration. Each assay was incubated for 45 min with EcGK and initiated by the addition of ATP to a final concentration of 2.5 mM. The lines show the fits to Equation 4.

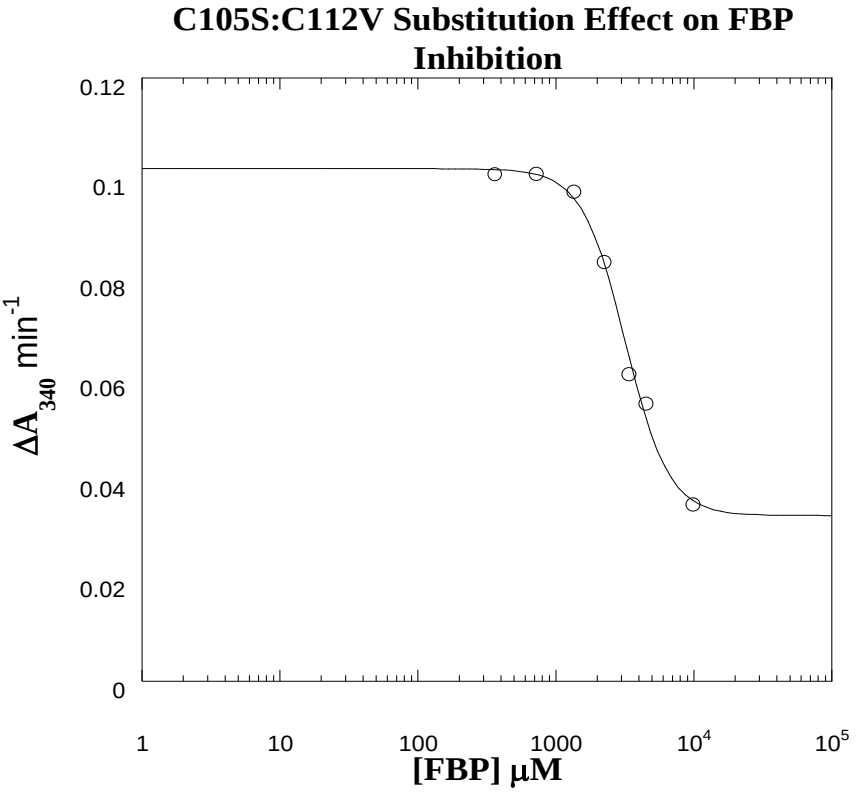

Figure 32: C105S:C112V Substitution Effect on FBP Inhibition. Each point on the graph indicates an individual assay conducted at the indicated FBP concentration. Each assay was incubated for 45 min with EcGK and initiated by the addition of ATP to a final concentration of 2.5 mM. The lines show the fits to Equation 4.

The effect of the substitutions on IIA^{glc} inhibition is in Figure 33 for C292S, C255S, and C269A, and Figure 34 for C105S:C112A and C105S:C112V. These plots were again generated using Kaleidagraph and Equation 5.

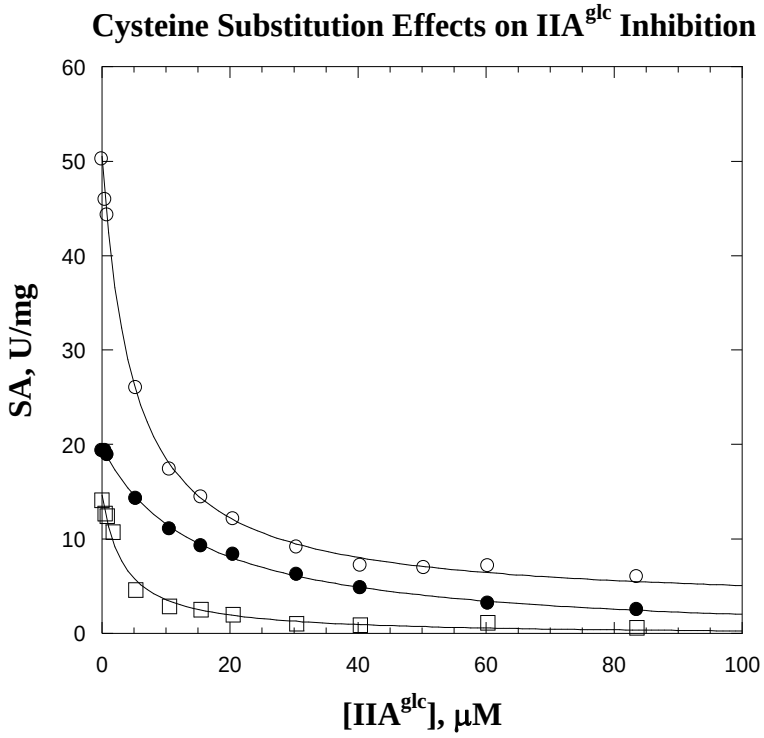

Figure 33: Cysteine Substitution Effects on IIA^{glc} Inhibition. Each point on the graph indicates an individual assay conducted at the indicated IIA^{glc} concentration. Each assay was initiated by the addition of EcGK to a final concentration as described previously. The open circles represent C292S, the filled circles represent C255S, and the open squares represent C269A. The lines show the fits to Equation 5.

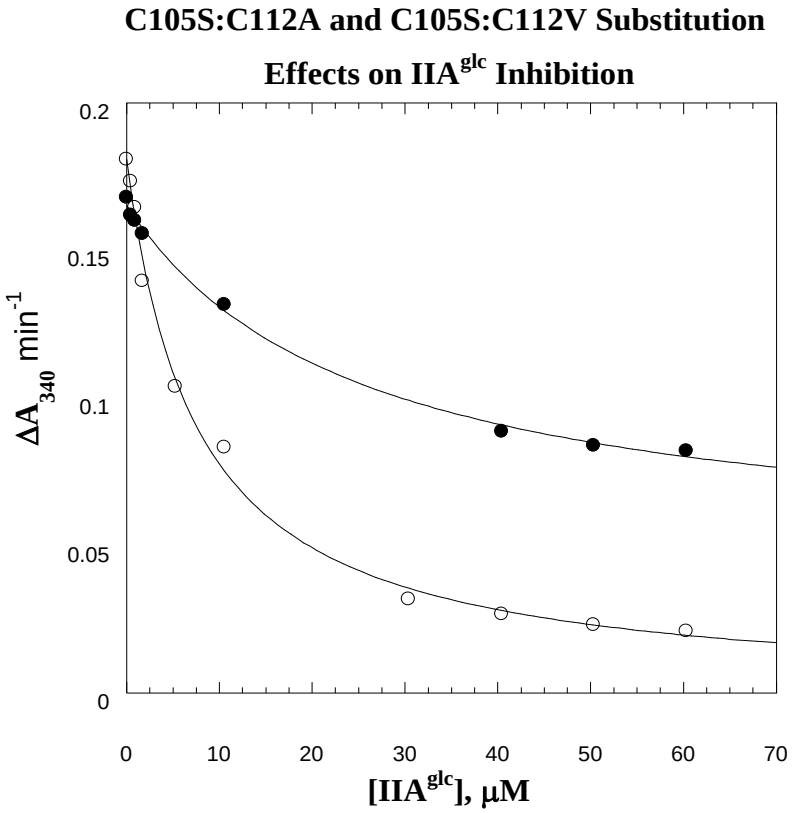

Figure 34: C105S:C112A and C105S:C112V Substitution Effects on IIA^{glc} Inhibition. Each point on the graph indicates an individual assay conducted at the indicated IIA^{glc} concentration. Each assay was initiated by the addition of EcGK to a final concentration as described previously. C105S:C112A is represented by the filled circles and C105S:C112V is represented by the open circles. The lines show the fits to Equation 5.

The results from Figures 27 through 34 are summarized below in Table 5. These parameters were all extracted to determine the effect of cysteine substitutions on the activity of EcGK.

Table 5: Cysteine Substitution Effects on the Functional Properties of EcGK

Parameter	ENZYME					
	Wildtype	**C292S**	**C255S**	**C269A**	**C105S: C112A**	**C105S: C112V**
	Glycerol Initial Velocity Studies					
V_{max}, U/mg	50 ± 1[b]	45 ± 1	23 ± 1	10 ± 1	ND	ND
K_m^{Gol}, µM	37 ± 4[b]	60 ± 8	12 ± 2	6 ± 2	ND	ND
	ATP Initial Velocity Studies					
V_{max}, U/mg	13 ± 5[b]	16 ± 1	4 ± 1	3 ± 1	ND	ND
K_m^{ATP}, µM	9 ± 2[a]	18 ± 2	6 ± 1	1.5 ± 0.3	ND	ND
	FBP Inhibition					
SA_0, U/mg	41 ± 2[a]	31 ± 2	12 ± 1	11 ± 1	UTD	UTD
$K_{0.5}^{FBP}$, µM	630 ± 90[a]	804 ± 149	190 ± 18	224 ± 10	423 ± 309	320 ± 22
W_{FBP}	0.02 ± 0.05[a]	0.02 ± 0.10	0.01 ± 0.02	0.02 ± 0.01	0.3 ± 0.3	0.3 ± 0.1
n_H	1.6 ± 0.3[a]	1.5 ± 0.5	1.8 ± 0.3	1.6 ± 0.1	0.8 ± 0.2	>2
	IIA^{glc} Inhibition					
SA_0, U/mg	36 ± 1[a]	51 ± 1	20 ± 1	15 ± 1	UTD	UTD
$K_{0.5}^{IIAglc}$, µM	6.3 ± 1[a]	5 ± 1	15 ± 1	3 ± 1	25 ± 5	8 ± 1
W_{IIAglc}	0.07 ± 0.04[a]	0.06 ± 0.01	0	0	0.2 ± 0.1	0

a: Values taken from Pettigrew (5)
b: Values taken from Acquaye (24)

The table compares the catalytic and functional properties of EcGK for each of the cysteine mutants. ND is not determined and UTD is unable to be determined. The parameters were extracted from fits to Equations 1-5.

The single cysteine mutants differed on catalytic parameters. The K_m^{Gol} is 2-fold higher for C292S, 3-fold smaller than wildtype for C255S, and 6-fold lower for C269A. For the K_m^{ATP}, there is a 2-fold difference between wildtype and C292S and a 9-fold difference between wildtype and C269A. As for V_{max}, the results were mirrored

between the initial velocity studies. According to the glycerol initial velocity studies, C255S V_{max} was 2-fold lower than wildtype and C269A V_{max} was 5-fold lower than wildtype. According to the ATP initial velocity studies, C255S V_{max} was 2-fold lower and C269A V_{max} was 3-fold lower than wildtype.

The inhibition parameters for the single cysteine mutants are also different in most cases. The $K_{0.5}^{FBP}$ is approximately 3-fold different for C255S and C269A compared to wildtype. With respect to IIA^{glc}, only C255S had a 2-fold difference in $K_{0.5}$ compared to wildtype. The W values from IIA^{glc} inhibition are zero for C255S and C269A, unlike the W of 0.07 for wildtype. The W_{FBP} is equivalent between wildtype and the single cysteine mutants.

Comparison of the dual cysteine mutants was done by analyzing EcGK that had only been purified by streptomycin sulfate and ammonium sulfate precipitation. Since the EcGK concentration could not be determined, the plots were generated by analyzing a change in A_{340} over time in the presence of different concentrations of inhibitor. The $K_{0.5}^{FBP}$ value for C105S:C112A was comparable to wildtype and that for C105S:C112V was 2-fold lower than wildtype. The W_{FBP} value for C105S:C112A is indistinguishable from wildtype because of the error margins, however, the value for C105S:C112V is at least 10-fold higher than wildtype. Furthermore, the n_H for C105S:C112A was close to 1 and indicates either no homotropic coupling for FBP binding or slightly antagonistic coupling. The $K_{0.5}^{IIAglc}$ was similar between wildtype and C105S:C112V, but it was 4-fold higher than wildtype for C105S:C112A. The W_{IIAglc} was 2-fold higher for C105S:C112A compared to wildtype and it was a value of zero for C105S:C112V.

CHAPTER V

DISCUSSION

E36C as a Suitable Model for Wildtype EcGK

The effect of the E36C substitution on the catalytic and allosteric properties of EcGK can be assessed from the results presented in Table 1. Comparison of the parameters shows that the substitution does not significantly affect the catalytic or allosteric properties of the enzyme.

Catalytic Parameter Comparison. The catalytic properties of E36C and wildtype EcGK are similar. In the initial velocity studies performed for determining activity dependence on glycerol and G3P concentration, the V_{max} for the forward direction was larger for E36C by a small amount. In the reverse direction, the V_{max} for E36C is less than that for wildtype by a small amount. The K_m^{Gol} and K_m^{G3P} values for E36C were somewhat smaller than those for wildtype. The heterotropic coupling assays yield values for V_{max} and K_m^{ATP}, and those obtained were similar with FBP and with IIA^{glc}. The V_{max} for the FBP and ATP/ADP coupling assays was larger for E36C in the forward direction and smaller in the reverse direction when compared to wildtype.

Although each set of experiments showed no difference in V_{max} between E36C and wildtype EcGK, there are differences between the initial velocity and heterotropic coupling experiments. The V_{max} in the forward direction was 3-fold larger in the initial velocity studies than the heterotropic coupling assays for both E36C and wildtype. These effects on V_{max} can be attributed to a difference in ATP concentration used for the

different experiments. For the initial velocity studies, the concentration of ATP used was 2.5 mM. For the heterotropic coupling studies, the concentration of ATP used was ≤100 μM. In the reverse direction, the initial velocity studies have only a small decrease in V_{max} compared to the coupling studies for both enzymes.

Comparison of the catalytic parameters for FBP heterotropic coupling and IIA^{glc} heterotropic coupling yields many similarities as well. The V_{max} for E36C in the forward direction as well as for wildtype and E36C in the reverse direction is equivalent between the FBP heterotropic coupling and IIA^{glc} heterotropic coupling experiments. Also similar between the experiments is the K_m^{ATP} and the K_m^{ADP} values. These values are all the same for both experiments. The only difference between the FBP coupling and IIA^{glc} coupling experiment is the wildtype V_{max} in the forward direction. Although there is less activity in the FBP heterotropic coupling experiment than that for the IIA^{glc} experiment, the difference is small. These results also support similarity between wildtype and E36C, as the methods produced parameters that were equivalent.

The results discussed above show that many of the catalytic parameters are the same for both wildtype and E36C and that any differences are small. Since there are no large effects on these parameters, the catalytic properties of EcGK are not significantly altered by cysteine substitution of E36. Thus, it appears that E36C is a fair representative of wildtype EcGK catalytic activity.

Comparing Allosteric Parameters. The allosteric properties of E36C and wildtype EcGK are similar for FBP inhibition as shown in the FBP inhibition studies. The specific activity in the absence of inhibitor for the FBP inhibition studies was

increased a small amount by the E36C substitution in the forward direction and not affected in the reverse direction. The $K_{0.5}^{FBP}$ is smaller for E36C than wildtype in the forward direction and larger for E36C than wildtype in the reverse direction. These differences were nominal. The W_{FBP} was equivalent between the two enzymes in the forward direction and 2-fold higher for E36C than wildtype. The n_H values are similar between both enzymes in both directions. Therefore, this experiment indicates that the enzymes are similar with respect to FBP binding and inhibition.

The allosteric properties of E36C and wildtype EcGK are also similar for the IIA^{glc} inhibition studies. The specific activity in the absence of inhibitor for the IIA^{glc} inhibition studies was increased by the E36C substitution in the forward direction and decreased by the substitution by a nominal amount in the reverse direction. As for the effect of the substitution on $K_{0.5}^{IIAglc}$, the E36C value is higher than wildtype by a small amount in the forward direction and 2-fold higher in the reverse. The W_{IIAglc} values are equivalent for both enzymes in both directions. Therefore, the enzymes are similar with respect to IIA^{glc} binding and inhibition.

The results of the heterotropic coupling assays for FBP and IIA^{glc} showed only small differences in the parameters for wildtype and E36C. In the FBP heterotropic coupling experiments, the $K_{0.5}^{FBP}$ was decreased by the E36C substitution in the forward direction and increased in the reverse. The parameters W, Q, and n_H are equivalent between wildtype and E36C in both reaction directions. In the IIA^{glc} heterotropic coupling experiments, the $K_{0.5}^{IIAglc}$ was equivalent between the two enzymes in the forward direction and affected by a small amount in the reverse direction. There is a

small increase in W_{IIAglc} for E36C in the forward direction, and the results are indistinguishable in the reverse. These results further support that the enzymes are equivalent with respect to FBP/IIA^{glc} binding and inhibition.

The parameters for E36C and wildtype for the inhibition studies showed no drastic effects from the substitution in these experiments, but there are differences between the parameters in different experiments. The specific activity for wildtype FBP inhibition in the forward direction was slightly larger than that for IIA^{glc} inhibition in the inhibition studies. This difference can be attributed to using a different enzyme preparation for each of these experiments. However, the specific activity values obtained from the inhibition studies for E36C in the forward direction was equivalent between the inhibition studies. Those for wildtype and E36C were also equivalent in the reverse direction.

Comparison of the inhibition and heterotropic coupling studies showed some differences in the parameters obtained for FBP inhibition by the different methods. For the forward direction, the $K_{0.5}^{FBP}$ from the inhibition studies is 4-fold higher for wildtype and 5-fold higher for E36C than the values from the heterotropic coupling experiments. The parameters obtained from the inhibition studies represent $K_{0.5}^{FBP}$ at the saturating presence of ATP (2.5mM) and those from the heterotropic coupling assays represent $K_{0.5}^{FBP}$ in the absence of ATP, i.e. K_{FBP}^{∞} and K_{FBP}^{0}, respectively. ATP concentration as the cause of the discrepancy is supported by the Q for FBP and ATP coupling being antagonistic ($Q<1$). This conclusion is supported by the agreements between the $K_{0.5}^{FBP}$ determined from the two experiments in the reverse direction, for which $Q=1$ for

FBP/ADP allosteric coupling. The W_{FBP} was equivalent between the two experiments for wildtype in both directions. The W_{FBP} for E36C is also similar in both the forward and reverse direction because $W_{FBP}<<1$ for both experiments. The n_H values were all equivalent for both enzymes between the experiments with the exception of E36C in the reverse direction. This difference, however, was small.

Comparison of the inhibition and heterotropic coupling studies showed more small differences in the parameters obtained for IIA^{glc} inhibition by the different methods. The $K_{0.5}^{IIAglc}$ was equivalent between the two methods for wildtype in the forward direction, 2-fold less for E36C in the forward direction, 2-fold higher for wildtype in the reverse direction, and only slightly different for E36C in the reverse direction for the heterotropic coupling experiments compared to the inhibition assays. The W_{IIAglc} was equivalent between the methods for both wildtype and E36C in the forward direction. The W_{IIAglc} for wildtype in the reverse direction is 2-fold less for the coupling experiments compared to the inhibition experiments, and the W for E36C is not different between the methods. The data therefore show that the methods all report similar parameters for IIA^{glc} binding and inhibition, providing further support for similarity between the enzymes.

The results discussed above show that many of the allosteric parameters are the same for both wildtype and E36C and that any observed differences are small. These differences are 2-fold or less, sometimes overlapping. Since the errors are represented here as standard errors, a 2-fold difference is not large enough to constitute a change in the allosteric properties of EcGK. This, in conjunction with the result from analyzing

the catalytic parameters, indicates that E36C is a fair representative of wildtype EcGK activity.

Effects of Labeling with Extrinsic Fluorophore on E36C Functional Properties

One approach to determine the molecular basis for allosteric control in EcGK is to monitor ligand binding. Labeled E36C may be a useful probe for reporting on the ligand-dependent conformational changes at the catalytic cleft. A caveat to using labeled E36C is that the labeling by 6IAF may interfere with the functional properties of the enzyme due to its large size and hydrophobicity. To address this issue, effects of fluorescein labeling to low stoichiometry on the specific activity and allosteric properties were determined. By considering the data in Table 2 and taking notice of the standard errors, it becomes apparent that most of the parameters either overlap or are close to one another in value. Small discrepancies are observed for the time zero and labeled E samples compared to the untreated samples. This is most likely due to the presence of quenched fluorophore in the sample since the untreated (no label) and labeled C (NAP-10 purified) samples had the same parameters. Since no effect is seen, it is possible that there is either no effect from labeling or that the effect is too small to be seen at 0.12 stoichiometry. It is possible that higher stoichiometries of label to EcGK subunits may amplify differences in the allosteric properties of the enzyme. This still needs to be addressed, however, all stoichiometries used in this work were kept below 0.12 to prevent homo-FRET (28) and the similarity between the untreated and labeled C

samples indicate that labeling does not visibly alter the functional properties of E36C at this stoichiometry.

The data in Table 2 shows that there is no effect on EcGK function from 6IAF labeling, but there are a few discrepancies when comparing the parameters between different experiments. First, the V_{max} values from these experiments are smaller than those from the earlier initial velocity studies and inhibition studies. However, the enzyme used is from a different preparation date and all the other parameters are comparable across the experiments with the exception of W_{FBP}. This W_{FBP} value obtained from this experiment is, however, comparable to the inhibition and heterotropic coupling studies previously performed because $W<<1$ and is only 2-fold higher than those from the inhibition studies. In addition, the rest of the parameters are comparable between experiments.

Effects of Catalytic Site and Allosteric Ligands on Fluorescence Anisotropy of Fluorescein-Labeled E36C EcGK

Stopped-flow experimentation is a possible approach for determining FBP and IIA^{glc} effects on the on- and off-rates of substrates. However, this method is only applicable if changes in fluorescence properties of the labeled enzyme are observed upon ligand binding. In Table 3, binding of substrates both individually and simultaneously affect the anisotropy of labeled E36C.

The fluorescence anisotropy is changed by substrate binding. Formation of the binary complexes of enzyme with either ATP, Gol, ADP, or G3P increases the

anisotropy. This indicates that the labeled E36C position is reporting on conformational effects of substrate binding. Formation of the ternary complexes of enzyme with either ATP and Gol or ADP and G3P increases the anisotropy to a greater extent than the binary complexes. Observation of an increased effect upon formation of the ternary complexes suggests that fluorescence is reporting on heterotropic coupling between substrates. This supports the heterotropic coupling between substrates that is indicated by the differences between the Michaelis constants and dissociation constants for both reaction directions for EcGK (36).

The fluorescence anisotropy is changed by binding of the allosteric inhibitors. Binding of IIA^{glc} to the binary and ternary complexes affects the anisotropy of labeled E36C. IIA^{glc} binding increases the anisotropy of the enzyme/ATP and enzyme/ADP binary complexes. Its effects on the anisotropy of the enzyme/Gol and enzyme/G3P binary complexes are not significant. IIA^{glc} binding decreases the anisotropy for the enzyme/ATP/Gol and enzyme/ADP/G3P ternary complexes. Titration of the EAB ternary complex showed that binding of IIA^{glc} is not affected by the concentration of ATP (Table 3).

It was shown that IIA^{glc} inhibition of wildtype EcGK and the variants E478C, E478C GVN, R369A, and A65T are all dominated by V-type control (5,18). For these enzymes, the effect of Q coupling for the substrates was approximately 2, indicating that binding of IIA^{glc} may be slight cooperative in the presence of ATP, but that its inhibition is a predominately V_{max}. An S58W variant that is insensitive to inhibition by FBP samples an open conformation visible by x-ray crystallography that brings the γ-

phosphate of ATP within 4.7Å of the O3 of glycerol (26), leading to the suggestion that this open conformation is the active form. This led to the proposal of FBP and IIA^{glc} inhibiting the enzyme by promoting the closed form that creates a distance of 7Å between the ATP and glycerol (26). Since heterotropic coupling is not observed for IIA^{glc} and nucleotides, it is possible that IIA^{glc} does not inhibit in this manner or that it affects the on- and off-rates of substrates equally. Titrations of the EAB ternary complex with IIA^{glc} and the reported Q values in Table 1 indicate, at most, weak coupling to ATP. It is also interesting to note that binding of IIA^{glc} to the binary complexes increased the anisotropy and yet binding to the ternary complex decreases anisotropy. This suggests that coupling is involved in IIA^{glc} binding and since its binding does not affect the enzyme/nucleotide binary complexes, it is possible that it may be coupled to Gol or G3P binding.

Binding of FBP to the binary and ternary complexes also affects the anisotropy of labeled E36C. FBP binding decreases the anisotropy of the enzyme/Gol and enzyme/G3P binary complexes. Its effects on the anisotropy of the enzyme/ATP and enzyme/ADP binary complexes are small and not significant. FBP binding decreases the anisotropy for the enzyme/ATP/Gol and enzyme/ADP/G3P ternary complexes. The titration of the EAB ternary complex at 2.5mM and 100 μM ATP illustrates a distinctive shift in the affinity for FBP binding (Figure 23 and Table 4). The $K_{0.5}^{FBP}$ is 5-fold larger at 2.5mM ATP than at 100 μM ATP. Also, the n_H at 2.5 mM ATP illustrates no FBP coupling, in contrast to positive cooperativity observed at 100 μM ATP.

Previous studies have shown that FBP displays characteristics of a V-type system with respect to glycerol since the inhibition constant for FBP is not dependent on glycerol concentration (13). In 1973, FBP was shown to be non-competitive (37). The experiments performed only used a single concentration of FBP to make the determinations. The results presented here for the fluorescence titrations of the EAB ternary complex clearly show antagonistic heterotropic coupling between FBP and ATP. This is further supported by the FBP inhibition parameters shown in Table 1 for ATP coupling where the Q value is 0.6 ± 0.2 and 0.4 ± 0.1 for wildtype and E36C, respectively. These data indicate that FBP/ATP coupling is antagonistic. Thus, inhibition by FBP in the forward direction is due to K-type inhibition in conjunction with V-type inhibition. As for ADP, its binding is not coupled to FBP according to Table 1, but an effect may not be visible because on- and off-rates are effected equally for ADP.

Addressing Q-Coupling Through Fluorescence. Fluorescence anisotropy can be used to determine ligand effects on the substrate on- and off-rates and to elucidate the effect of ligands on binding and determine the extent of Q-coupling. The data in Table 3 shows that coupling can be performed for FBP and ATP by titrating the enzyme/Gol complex with ATP and the enzyme/Gol/FBP complex with ATP. This also works for FBP and Gol coupling by titrating the enzyme/ATP complex with glycerol and then titrating the enzyme/ATP/FBP complex with glycerol. To assess coupling between FBP and ADP or FBP and G3P, titrations can be performed as follows: enzyme/G3P titrated with ADP and enzyme/G3P/FBP titrated with ADP for FBP/ADP coupling;

enzyme/ADP titrated with G3P and enzyme/ADP/FBP titrated with G3P. The applicability of this method is supported by the results shown in Table 4 for FBP binding to the EAB ternary complex. Since it was possible to see antagonistic coupling between FBP and ATP, it is possible to determine coupling with other ligands using fluorescence.

Coupling can also be performed for IIA^{glc} and the substrates. To assess coupling between IIA^{glc} and ATP, ADP, Gol, and G3P, the following titrations can be performed: enzyme/Gol titrated with ATP and enzyme/Gol/IIA^{glc} titrated with ATP; enzyme/ATP titrated with Gol and enzyme/ATP/IIA^{glc} titrated with Gol; enzyme/G3P titrated with ADP and enzyme/G3P/IIA^{glc} titrated with ADP; enzyme/ADP titrated with G3P and enzyme/ADP/IIA^{glc} titrated with G3P.

The changes in anisotropy for the binary and ternary complexes with and without IIA^{glc} show promise for determining Q-coupling by fluorescence. The only caveat for determining Q-coupling for IIA^{glc} and substrates with this method is that the ternary complexes in Table 4 show different $K_{0.5}$ values for IIA^{glc} than those observed from the inhibition studies in Table 1. The IIA^{glc} titration of the EAB ternary complex produces a $K_{0.5}^{IIAglc}$ that is 2-fold higher than the value obtained from the IIA^{glc} inhibition studies. The IIA^{glc} titration of the EPQ ternary complex produces a $K_{0.5}^{IIAglc}$ that is 4-fold higher than the value obtained from the IIA^{glc} inhibition studies. Although these values are not equivalent, they are still similar and may only be different because of the absence of Mg^{2+}. If Mg^{2+} is the reason for the difference among the data, it would appear as though Mg^{2+} affects IIA^{glc} binding but not FBP.

Native Cysteines as Probes for Monitoring EcGK Conformational Changes

The long term goal for analyzing the effect of the cysteine substitutions is so that the cysteines can be identified in an NMR spectrum and be used as reporters of ligand binding. To determine which cysteines are potential reporters, the effects of substitutions at these cysteine positions on the catalytic and allosteric properties of EcGK were determined. Since the data show they do elicit some effect on the properties of EcGK, it indicates that these positions will report on conformational changes within the protein

According to the data in Table 3, every parameter from initial velocity and inhibition studies is affected by at least one of the mutants analyzed. Both C292S and C269A affected the K_m^{ATP} and all three single substitutions affected the K_m^{Gol}. C255S and C269A affected $K_{0.5}^{FBP}$, the dual substitutions affected W_{FBP}, C255S, C269A and C105S:C112A affected $K_{0.5}^{IIAglc}$, and all but C292S affected W_{IIAglc}. Thus, all of these mutants can theoretically report on ligand binding and have their environmental changes monitored by NMR.

In summary, either C292S or C269A would report on ATP binding and all the single substitutions could be used to probe glycerol binding. C255S and C269A would report on FBP binding and the dual mutants would show conformational changes from FBP exerting inhibition. C255S, C269A and C105S:C112A would report on IIA^{glc} binding and all the mutants would report on conformational changes from IIA^{glc} inhibition (with the exception of C292S). The only issue with using these proteins is their instability. The single cysteine mutants were only stable for a short time after the

third column and the double cysteine mutants would not retain activity if put on the first column. Since the samples would need to be pure and highly concentrated for NMR spectroscopy, new protein isolation or purification protocols need to be developed.

CHAPTER VI

CONCLUSIONS

The results of this study provide new insights into regulation of EcGK by FBP and IIA^{glc} and establish a foundation for probing the mechanism of regulation for this novel enzyme. Inhibition for both directions was characterized as either K-type or V-type for both FBP and IIA^{glc}. It was also shown that E36C is a suitable model for wildtype activity and that fluorescence can be used to monitor binding of ligands. Finally, the results show that the native cysteines will provide structural information that may be viewed by shifts in an NMR spectrum.

From the heterotropic coupling experiments it is clear that inhibition by IIA^{glc} in both the forward and reverse direction can be attributed to V-type inhibition. As for FBP inhibition, the effect is K-type and V-type for the forward direction and V-type for the reverse. These conclusions are further supported by the fluorescence titrations explained previously.

Due to the fluorescence studies, it is now known that changes in the E36 environment occur upon ligand binding because of the bound fluorophore response. Since fluorescence titrations were performed in this work and produced workable $K_{0.5}$ values for the inhibitors, there is promise for Q-coupling determination. Thus, further characterization of the on and off rates of substrates and the effect FBP and IIA^{glc} have on those rates is now possible by use of stopped-flow. Most importantly, however, use

of E36C provides an amiable alternative to wildtype, enabling a clearer depiction of the natural protein's catalytic process.

Characterization of the cysteine substitutions provides a platform for studying environmental changes in response to ligand association by NMR. Each of the substitutions tested contributes to the study by affecting at least one catalytic and allosteric parameter. Thus, these positions may report upon ligand binding.

REFERENCES

1. Hurley, J. H. (1996) *Annual Review of Biophysics and Biomolecular Structure* **25**, 137-162

2. Gerstein, M. (1994) *Biochemistry* **33**, 6739-6749

3. Grueninger, D. (2006) *Journal of Molecular Biology* **359**, 787-797

4. Bennett, W. S., and Steitz, T. A. (1980) *Journal of Molecular Biology* **140**, 211-230

5. Pettigrew, D. W. (2009) *Archives of Biochemistry and Biophysics* **492**, 29-39

6. Freedberg, W. B. (1973) *Journal of Bacteriology* **115**, 816-823

7. Miki, K., Silhavy, T. J., and Andrews, K. J. (1979) *J. Bacteriol.* **138**, 268-269

8. Lin, E. C. C. (1976) *Annual Review of Microbiology* **30**, 535-578

9. Phibbs, P. V., Jr., McCowen, S. M., Feary, T. W., and Blevins, W. T. (1978) *J. Bacteriol.* **133**, 717-728

10. Freedberg, W. B. (1971) *Journal of Bacteriology* **108**, 137-144

11. Zwaig, N. (1970) *Journal of Bacteriology* **102**, 753-759

12. Blattner, W. A., Knowles, J.R. (1979) *Biochemistry*, 3927-3933

13. Zwaig, N. (1966) *Science* **153**, 755-757

14. Lin, E. C. C. (1996) *Escherichia coli* and *Salmonella,* in *Cellular and Molecular Biology* (Ed.), F. C. Neidhardt ed., ASM Press, Washington D.C. pp 307-342

15. Hurley, J. H. (1993) *Science* **259**, 673-677

16. Novotny, M. J. (1985) *Journal of Bacteriology* **162**, 810-816

17. Yu, P. (2007) *Biochemistry* **46**, 12355-12365

18. Pettigrew, D. W. (2009) *Archives of Biochemistry and Biophysics* **481**, 151-156

19. Monod, J., Changeux, J.-P., and Jacob, F. (1963) *Journal of Molecular Biology* **6**, 306-329

20. Monod, J., Wyman, J., and Changeux, J.-P. (1965) *Journal of Molecular Biology* **12**, 88-118

21. Goodey, N. M. (2008) *Nature Chemical Biology* **4**, 474-482

22. Clarkson, M. W. (2006) *Biochemistry* **45**, 7693-7699

23. Suel, G. M. (2003) *Nature Structural Biology* **10**, 59-69

24. Acquaye, E. A., Pettigrew, D.W. (2011), Unpublished Lab Data, Department of Biochemistry and Biophysics, Texas A&M University, College Station.

25. Yeh, J. I., Charrier, V., Paulo, J., Hou, L. H., Darbon, E., Claiborne, A., Hol, W. G. J., and Deutscher, J. (2004) *Biochemistry* **43**, 362-373

26. Bystrom, C. E. (1999) *Biochemistry* **38**, 3508-3518

27. Anderson, M. J., DeLaBarre, B., Raghunathan, A., Palsson, B. O., Brunger, A. T., and Quake, S. R. (2007) *Biochemistry* **46**, 5722-5731

28. Yu, P. (2003), *Allosteric Regulation of Glycerol Kinase: Fluorescence and Kinetics Studies.* Ph.D. Dissertation. Texas A&M University, College Station

29. Pettigrew, D. W.(2011), Unpublished Lab Data, Department of Biochemistry and Biophysics, Texas A&M University,

30. Wuthrich, K. (1998) *Nature Structural Biology* **5**, 492-495

31. Pelton, J. G. (1991) *Proceedings of the National Academy of Sciences of the United States of America* **88**, 3479-3483

32. Stewart, G., Lubinskymink, S., Jackson, C. G., Cassel, A., and Kuhn, J. (1986) *Plasmid* **15**, 172-181

33. Pettigrew, D. W., Meadow, N. D., Roseman, S., and Remington, S. J. (1998) *Biochemistry* **37**, 4875-4883

34. Pettigrew, D. W. (1990) *Biochemistry* **29**, 8620-8627

35. Pettigrew, D. W. (1986) *Biochemistry* **25**, 4711-4718

36. Pettigrew, D. W. (1987) *Biochemistry* **26**, 1723-1727

37. Thorner, J. W., and Paulus, H. (1973) *J. Biol. Chem.* **248**, 3922-3932

VITA

Name: Shanna Quinn Mayorov

Address: Department of Biochemistry and Biophysics, c/o Dr. Donald Pettigrew, Texas A&M University, College Station, TX, 77843-2128

Email Address: slquinn7@tamu.edu

Education: B.S., Chemistry, Bloomsburg University, 2009

M.S., Biochemistry, Texas A&M University, 2011